4 Investigation of substituent effect on carbene ligands

4.1 Introduction

4.1.1 Background

After the initial recognition and first full characterization of a transition metal carbene complex by Fischer in 1964,[1] interest in divalent carbon as part of a metal system expanded quickly. Four years later the first of the so-called N-heterocyclic carbene (NHC) complexes were synthesized by Wanzlick,[2] followed shortly by the publication of another stable diaminocarbene metal complex by Öfele.[3] In an effort to prepare a homoleptic tantalum(V) alkyl complex, the first nucleophilic carbene metal complex was reported by Schrock six years later.[4]

Classification of the types of carbene complexes (Figure 4.1) was based on their unique characteristics. The carbene carbon atom of Fischer carbene complexes was found to be electrophilic, in contrast to Schrock carbene complexes. On the other hand, NHC's were initially seen as being a specific type of Fischer carbene, however significant differences qualified these types of complexes as a separate subclass of carbene complexes. As an example, the metal-carbon bond in Fischer and Schrock carbenes display double bond character while the

[1] Fischer, E.O.; Maasböl, A. *Angew. Chem., Int. Ed. Engl.* **1964**, *3*, 580.
[2] Wanzlick, H.W.; Schoenherr, H.J. *Angew. Chem., Int. Ed. Engl.* **1968**, *7*, 141.
[3] Öfele, K. *J. Organomet. Chem.* **1968**, *12*, 42.
[4] Schrock, R.R. *J. Am. Chem. Soc.* **1974**, *96*, 6796.

longer M-C bond lengths of NHC's (of the corresponding central metals), are classified as single bonds.[5]

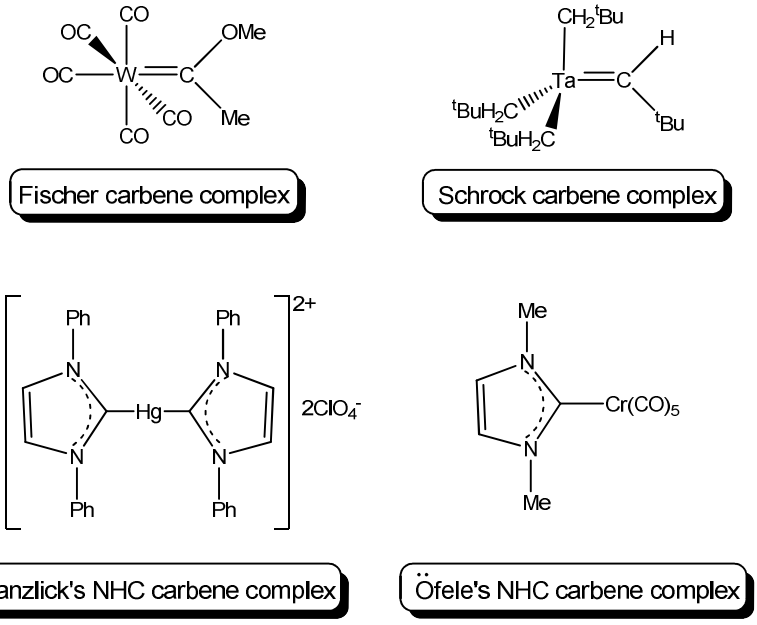

Figure 4.1 The first carbene complex to be synthesized in each of the three classes

General characteristics for carbene carbon atoms were found to be approximate sp^2 hybridization and trigonal planar geometry around the carbon atom.[6] However, Schrock carbene complexes are usually characterized by an early transition metal in high oxidation state as the central metal, with strong donor and weak π-acceptor ligands,[7] while the electrophilic Fischer carbene complexes contain predominantly low valent Group VI – VIII transition metals stabilized by π-acceptor ligands.[8]

[5] Herrmann, W.A. *Angew. Chem., Int. Ed. Engl.* **2002**, *41*, 1290.
[6] Elschenbroich, Ch.; Salzer, A. *Organometallics: a concise introduction 2nd edition,* **1992**, Verlagsgesellschaft, New York.
[7] (a) Schwab, P.; France, M.B.; Ziller, J.W.; Grubbs, R.H. *Angew. Chem., Int. Ed. Engl.* **1995**, *34*, 2039, (b) Scwab, P.; Grubbs, R.H.; Ziller, J.W. *J. Am. Chem. Soc.* **1996**, *118*, 100.
[8] Dötz, K.H.; Fischer, H.; Hofmann, P.; Kreissl, F.R.; Schubert, U.; Weiss, K. *Transition Metal Carbene Complexes,* VCH Verlag Chemie, Weinheim, **1983**.

The main speciation of the different types of carbene complexes are made by the nature of the metal-carbon bond, which in turn is influenced by the types of substituents bonded to the carbene carbon atom. Fischer carbene complexes contain at least one heteroatom bonded directly to the carbene carbon atom and NHC's have two N-atoms as α-substituents on the carbene carbon. Metal alkylidene, or Schrock carbene complexes, on the other hand, typically have alkyl- or H-atoms as carbene carbon atom substituents.

4.1.2 Theoretical bonding model of carbene ligands

The generally accepted bonding model employs the singlet and triplet states of the ground state spin multiplicities of the fragments CR_2 and L_nM as building blocks for carbene complexes.[9] For Fischer carbene complexes, the model describes the metal-to-carbon bond in terms of 'donor-acceptor interactions' between a ($^1A_1$) singlet carbene and a singlet metal fragment.[10] Carbene ligands with π-donor groups and a singlet ground state will preferentially engage in donor-acceptor interactions with singlet metal fragments.[11] In particular, dihalocarbenes, which have singlet ground states and large singlet to triplet excitation energies, are considered to be donor-accepting bonding and thus 'Fischer-type'. The resulting electrophilic carbene carbon can be considered as a neutral 2-electron ligand (LZ-type as described by Green's ligand classification method[12]). Applying the Dewar-Chatt-Duncanson (DCD) model[13] to describe the synergic interaction of the Fischer carbene bond, the primary interaction can be seen as the σ-donation from the sp^2 orbital of the carbene carbon atom to the metal σ-hybrid orbital, and π-backdonation from the metal *d*-orbital to the empty *p*-orbital of the carbene carbon atom.

[9] Bourissou, D.; Geurret, O.; Gabbaï, F.P.; Bertrand, G. *Chem. Rev.* **2000**, *100*, 39.
[10] Dötz, K.H. *Metal carbenes in organic synthesis*, Springer-Verlag, Germany, **2004**.
[11] Marquez, A.; Sanz, J.F. *J. Am. Chem. Soc.* **1992**, *114*, 2903.
[12] Green, M.L.H. *J. Organomet. Chem.* **1995**, *500*, 127.
[13] (a) Casey, C.P.; Boggs, R.A.; Anderson, R.L. *J. Am. Chem. Soc.* **1972**, *94,* 8947, (b) Weiss, K.; Fischer, E.O. *Chem. Ber.* **1973**, *106*, 1277.

Bonding in Schrock complexes are described as a covalent bond between a $^3B_1$ triplet carbene and a triplet metal fragment,[14] implying that the electronic ground state of a carbene ligand can be used to predict binding interactions with a transition metal.

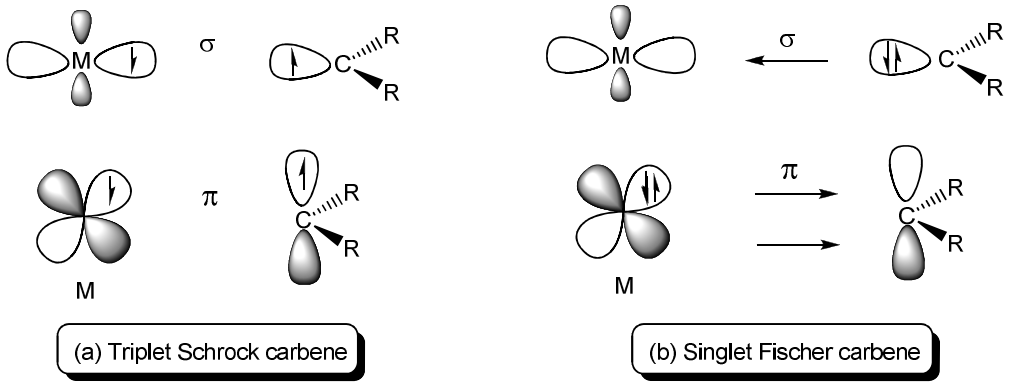

Figure 4.2 Orbital interactions of (a) Schrock and (b) Fischer carbene ligands

The neutral description of the Schrock carbene (Figure 4.2) can also be rewritten as the nucleophilic form L_nM^+-CR_2^- to explain the experimental observations that the Schrock carbene compounds react mostly as nucleophiles. A partial negative charge resides on the carbene carbon atom as a result of polarization of shared electrons between an electropositive metal and a more electronegative carbene carbon atom, as no heteroatom resides in the α-position for stabilization. The carbene ligand is therefore formally considered as an X_2-type ligand, resulting in electron sharing in a metal-carbon σ- and π-bond.

In Fischer and Schrock carbene complexes the *p*-orbital of the carbene is used for backbonding to the metal but in NHC's this *p*-orbital is used for backbonding from the adjacent nitrogen atoms.[15] Thus, only the σ-component is present in

[14] Cundari, T.R.; Gordon, M.S. *J. Am. Chem. Soc.* **1991**, *113*, 5231.
[15] Tafipolsky, M.; Scherer, W.; Öfele, K.; Artus, G.R.J.; Herrmann, W.A.; McGrady, G.S. *J. Am. Chem. Soc.* **2002**, *124*, 5865.

the M-C bond in NHCs and the negligible π-backbonding[16] is confirmed and verified with recent charge-density studies. As a result of this, NHC's can rotate around the M-C axis.

4.2 Molecular modelling

Molecular modelling is used to assist with prediction and confirmation of many aspects of experimental chemistry. The goal of the interpretative theoretical research is to present models which can help to qualitatively understand and predict the structures and reactivities of molecules. If the theory is an acceptable description of the system of interest, considerable information can be obtained theoretically. The model should also form a bridge between the chemical behaviour of a molecule and the underlying physical laws.

4.2.1 The theoretical method

Two main methods are used in molecular modelling: molecular mechanics (MM), which is based on the laws of classical physics, and the electronic structure method, which is based on quantum mechanics.[17] The latter can be divided into semi-empirical, *ab initio* and density functional theory (DFT). The DFT method is the most widely used, taking the effects of electron correlation into account. Although the DFT method is very similar to the *ab initio* Hartree-Fock (HF) method, the electron in the latter method is assumed to interact with an averaged electron density.[17] In the DFT method, the electronic energy can be seen as a summation of the electrons' kinetic energy, the potential energy of the nuclear electron interaction, the electron-electron repulsion energy and an exchange correlation term that describes the rest of the electron-electron interactions. The exchange correlation term is a functional of the electron

[16] Frenking, G.; Solà, M.; Vyboischchikov, S.F. *J. Organomet. Chem.* **2005**, *690*, 6178.
[17] Foresman, J.B.; Frisch, Æ. *Exploring Chemistry with Electronic structure methods,* 2nd Ed., Gaussian Inc., Pittsburgh, **1996**.

density function, and can be separated into the exchange and correlation functionals.

A pure DFT functional is usually defined by pairing an exchange functional with a correlation functional as in the case of the B3LYP functional where a Becke (B) defined functional is combined with a Lee-Yang-Parr (LYP) functional.[18]
For a theoretical calculation it is also necessary to describe mathematically the orbitals that combine to approximate the total electronic wavefunction of the system under investigation. Better orbital description implies larger basis sets, which leads to longer calculation times being required.

4.2.2 Molecular modelling of transition metal complexes

The progress in quantum chemical methods for the calculation of electronic structure has given insight into the nature of the chemical bond in transition metal carbene complexes. The paper published by Frenking and Frölich gave a comprehensive overview of the methods and approaches of computational chemistry as applied to the bonding in transition metal compounds.[19] Due to the advances in modern and well-defined quantum chemical charge and energy partitioning methods, it is now possible to study complex organometallic systems. Methods include atoms in molecules (AIM),[20] charge decompostition analysis (CDA),[21] energy decomposition analysis (EDA)[22] and natural bond orbital analysis (NBO).[23] The methods provide quantitative answers to questions regarding the bonding situation in terms of simple bonding models. Specifically, the NBO method gives a quantitative interpretation of the electronic structure of

[18] Becke, A.D. *Phys. Rev.* **1988**, *A38,* 3098.
[19] Frenking, G.; Fröhlich, N. *Chem. Rev.* **2000**, *100*, 717.
[20] Bader, R.F.W. *Atoms in Molecules: A Quantum Theory,* Oxford University Press, **1990**.
[21] (a) Dapprich, S.; Frenking, G. CDA 2.1, Marburg, **1994**, (b) Dapprich, S.; Frenking, G. *J. Phys. Chem.* **1995**, *99*, 9352.
[22] (a) Ziegler, T.; Rauk, A.; *Inorg. Chem.* **1979**, *18*, 1755, (b) Bickelhaupt, F.M.; Nibbering, N.M.M.; van Wezenbeek, E.M.; Baerends, E.J. *J. Phys. Chem.* **1992**, *96*, 4864, (c) Ziegler, T.; Rauk, A. *Inorg. Chem.* **1979**, *18*, 1558, (d) Ziegler, T.; Rauk, A. *Theor. Chim. Acta* **1977**, *46*, 1 (e) Kitaura, K.; Morokuma, K. *Int. J. Quantum Chem.* **1976**, *10*, 325.
[23] (a) Foster, J.P.; Weinhold, F. *J. Am. Chem. Soc.* **1980**, *102*, 7211, (b) Reed, A.E.; Weinhold, F.J. *J. Chem. Phys.* **1985**, *83*, 1736, (c) Reed, A.E.; Weinstock, R.B.; Weinhold, F. *J. Chem. Phys.* **1985**, *83*, 735, (d) Reed, A.E.; Curtiss, L.A.; Weinhold, F. *Chem. Rev.* **1988**, *88,* 899.

a molecule in terms of Lewis structures. Since Lewis structures are popular representations, the NBO method is frequently chosen. NBO analysis also has the advantage that results are quite robust against changing the basis set.[19]

The EDA method of bonding analysis focuses on the instantaneous interaction energy of the bond, which is the energy difference between the molecule and the fragments in the frozen geometry of the compound.[22] Dapprich and Frenking's CDA method[21] can be seen as a quantitative expression of the Dewar-Chatt-Duncanson (DCD) model[24] of the synergistic metal-ligand bonding, which considers the ligand→metal σ-donation and ligand←metal π-backdonation as the dominant factors of the metal-ligand bond.

4.2.3 Modelling of Fischer carbene complexes

Recently, various aspects of reactivities and properties of Fischer carbene complexes have been theoretically investigated by means of DFT calculations.[25] For example, the nature of the bonding of the metal-carbon bond in complexes was investigated by Frenking *et al.*[25(c)] Charge and energy decomposition analyses were carried out for 16 valence electron (VE) compounds $[Ru(PMe_3)_2Cl_2(C)]$ and $[Fe(PMe_3)_2Cl_2(C)]$; and 18VE compounds $[M(PMe_3)_2(CO)_2(C)]$ and $[M(CO)_4(C)]$ (M = Ru; Fe). The bonding analysis showed that 16 VE carbon complexes were much more stabilized by metal-carbon σ-interaction than 18 VE complexes. EDA calculations illustrated that the nature of the transition metal – carbon and the transition metal–carbonyl binding interactions resemble each other, and that the π-bonding contribution to the orbital energies in the 18 VE carbon complexes is always stronger than σ-

[24] (a) Dewar, M.J.S. *Bull. Soc. Chim. Fr.* **1951**,*18*, C79, (b) Chatt, J.; Duncanson, L.A. *J. Chem. Soc.* **1984**, *106*, 1576.
[25] (a) Cases, M.; Frenking, G.; Duran, M.; Sol, M.; *Organometallics* **2002**, *21*, 4182, (b) Krapp, A.; Frenking, G.; *J. Am. Chem. Soc.* **2008**, *130*, 16646, (c) Krapp, A.; Pandey, K.K.; Frenking,G. *J. Am. Chem. Soc.* **2007**, *129*, 7596, (d) Frenking, G.; Sola, M.; Vyboishchikov, S.F. *J. Organomet. Chem.* **2005**, *690*, 6178, (e) Sierra, M.A.; Fernández, I.; Cossío, F.P. *Chem. Commun.* **2008**, 4761, (f) Lage, M.L.; Fernández, I.; Mancheño, M.J.; Sierra, M.A. *Inorg. Chem.* **2008**, *47*, 5253, (g) Andrada, D.M.; Zoloff Michoff, M.E.; Fernández, I. Granados, A.M.; Sierra, M.A. *Organometallics* **2007**, *26*, 5854.

bonding. The properties of carbon complexes as donor ligands, and the nature of the donor-acceptor interactions with Lewis acids were also studied.[25(b)]

Studies of the steric and electronic effects of the heteroatom (S and O) on free carbenes and their metal complexes were carried out by the group of Sierra.[26] Carbenes can exist in two conformations, either *syn* or *anti* (Figure 4.3), and a clear bias for the *anti*-isomer of the free alkoxycarbenes were found.

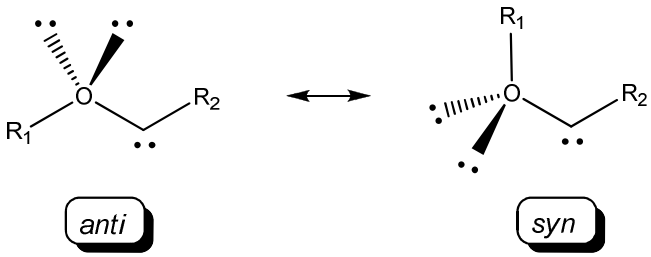

Figure 4.3 Possible conformations of carbene carbon heteroatom subsitituent

This was ascribed to the unfavourable steric repulsion between the substituent directly bonded to the heteroatom and the carbene carbon substituent of the *syn*-isomer, as well as the electronic repulsive interaction between the carbene electron pair and the two nonbonding electron pairs of the oxygen. For metal-complexed Fischer carbene ligands, only steric effects needed to be considered in the absence of the free carbene electron pair. Validation of the model was obtained in the observation of decreased differences of energies between the preferred *anti*- and *syn*-isomer.

Extensive studies, including molecular modelling, on reactivity and reaction mechanisms of thermal and photochemical transformations of Fischer carbene complexes have also been carried out by the aforementioned research

[26] Fernández, I.; Cossío, F.P.; Arrieta, A.; Lecea, B.; Mancheño, M.J.; Sierra, M.A. *Organometallics* **2004**, *23*, 1065.

group.[25(e), 27] It was found that the isolobal analogy[28] between Group VI Fischer carbene complexes and organic esters or amides holds for reactions occurring outside the participation of the metal. However, when the metal is directly involved in the reaction, the isolobal analogy should be excluded.

Other properties calculated include dipole moments, where recently it was found that the incorporation of two different metal fragments at the termini of a heteronuclear biscarbene complex, created a polarization effect comparable to that of a monocarbene complex, as illustrated in Figure 4.4.[29]

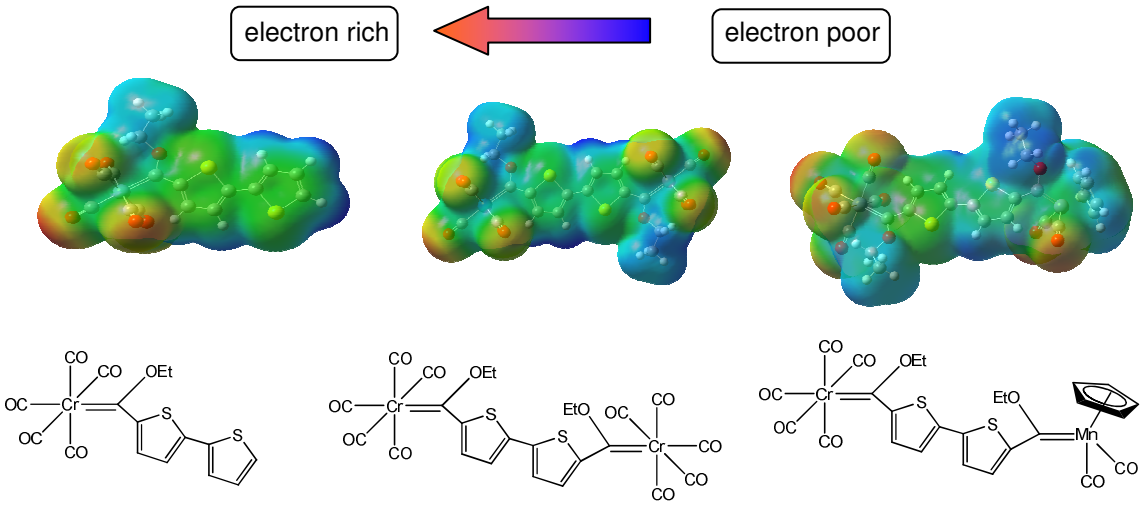

Figure 4.4 Electrostatic surface potentials mapped with total density of the molecule[29]

[27] (a) Fernández, I.; Sierra, M.A.; Mancheño, M.J.; Gómez-Gallego, M.; Cossío, F.P. *J. Am. Chem. Soc.* **2008**, *130*, 13892, (b) Fernández, I.; Sierra, M.A.; Mancheño, M.J.; Gómez-Gallego, M.; Cossío, F.P. *Eur. J. Chem.* **2008**, 2454, (c) Fernández, I.; Sierra, M.A.; Gómez-Gallego, M.; Mancheño, M.J.; Cossío, F.P. *Chem. Eur. J.* **2005**, *11*, 5988, (d) Arrieta, A.; Cossío, F.P.; Fernández, I.; Gómez-Gallego, M.; Lecea, B.; Mancheño, M.J.; Sierra, M.A. *J. Am. Chem. Soc.* **2000**, *122*, 11509.

[28] (a) Hoffmann, R. *Science* **1981**, *211*, 995, (b) Hoffmann, R. *Angew. Chem., Int. Ed. Engl.* **1982**, *21*, 711.

[29] Landman, M.; Ramontja, J.; van Staden, M.; Bezuidenhout, D.I.; van Rooyen, P.H.; Liles, D.C.; Lotz, S. *Inorg. Chim. Acta* **2010**, *363*, 705.

4.2.4 Substituent effect

Besides the above properties, quite a few theoretical investigations have focused on the effect of substituents on the carbene ligand. Several studies have shown that the chemical reactivity of the Fischer-type Cr-carbene complexes [$Cr(CO)_5${C(X)R}] depends mainly on the electronic characteristics of the carbene substituents X and R, which seem to have remarkable control on the electrophilicity of the complex.[30] Specifically, it has been proposed that the π-bond character of a metal carbene can be better represented by a M-C-X 3-centre, 4-electron bond.[31] For complexes where substituent X is a heteroatomic substituent (ethoxy, amino or thiophenol) and R a heteroaromatic substituent (furyl, thienyl and *N*-methylpyrryl), spectroscopic studies including IR, UV and NMR spectroscopy were directed at the investigation of the electronic properties of these complexes, specifically the donation of electron density from X and R into the empty *p* orbital on the carbene carbon.[32] It was concluded that stabilization occurs by conjugative release of electrons from the heteroarene substituent R rather than specific π → *p* donation, and that the electronic character of the carbene carbon atom is more strongly influenced by the X group than either the metal or the R group.

Poater *et al.* similarly found that donation from the carbene ligand is stronger than backdonation from the $Cr(CO)_5$-fragment.[33] However, they found that it is backdonation rather than σ-donation that correlates with most geometrical and electronic parameters of the complexes. Charge backdonation values and π-orbital interaction energies are more scattered over a large range of values, while charge donation values and σ-orbital interaction energies are more constant. Additionally, it was found that the smaller the π-donor character of X,

[30] (a) Dötz, K.H. *Angew. Chem., Int. Ed. Engl.* **1975**, *14*, 644, (b) Bernasconi, C.F.; Ali, M.; Lu, F. *J. Am. Chem. Soc.* **2000**, *122*, 2183.
[31] (a) Wang, C.-C.; Wang, Y.; Liu, H.-J.; Lin, K.-J.; Chou, L.-K.; Chan, K.-S. *J. Phys. Chem. A* **1997**, *101*, 8887, (b) Block, T.F.; Fenske, R.F. *J. Am. Chem. Soc.* **1977**, *99*, 4321.
[32] (a) Connor, J.A.; Jones, E.M. *J. Chem. Soc. A, Inorg. Phys. Theor.* **1971**, *12*, 1974, (b) Connor, J.A.; Jones, E.M.; Randall, E.W.; Rosenburg, E. *J. Chem. Soc., Dalton Trans.* **1972**, *22*, 2419.
[33] Poater, J.; Cases, M.; Fradera, X.; Duran, M.; Solà, M. *Chem. Phys.* **2003**, *294*, 129.

the larger the backdonation from the metal. In general, it was found that backdonation, as defined in the CDA[21] and EDA[22] methods, is proportional to the Cr-CO_{trans} distance, and inversely proportional to the Cr-C(carbene) and C-O(*trans*) distances. Therefore, the π-donor character of the X-substituent has the largest impact on the electron delocalization between the Cr, C(carbene) and X atoms. Substituents with a high π-donor character will lead to a decrease in electron sharing between C(carbene) and X.

Other properties of carbene complexes have also been used as a gauge of substituent effect on molecular structure and bonding. The groups of Frenking[34] and Goldman[35] have found that when comparing the carbonyl stretching frequencies of $[M(CO)_nL]$ systems, higher or lower values of ν(CO) does not necessarily indicate stronger or weaker π-acceptance of L. σ-bonding and charge interactions also have a significant influence, therefore a more legitimate correlation between the bonding situation and the force constants, rather than the vibrational frequencies, can be made.

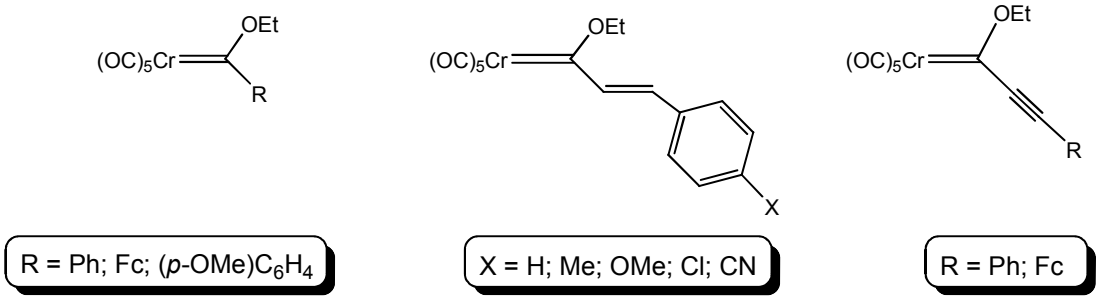

Figure 4.5 Alkoxycarbene chromium(0) complexes studied by TD-DFT[25(f)]

A computational time-dependent density functional theory (TD-DFT) experimental study of UV-visible spectroscopy of alkoxycarbene chromium(0) complexes (Figure 4.5) has been carried out to accurately assign the vertical transitions responsible for observed spectra.[25(f)] Ferrocene was included as a

[34] Lupinett, A.J.; Fau, S.; Frenking, G.; Strauss, S.H. *J. Phys. Chem. A* **1997**, *101*, 9551.
[35] Goldman, A.S.; Krogh-Jesperson, K. *J. Am. Chem. Soc.* **1996**, *118*, 12159.

substituent to investigate the effect of an additional metal atom on the electronic properties of Fischer carbenes.

Both the ligand field (LF) and metal-to-ligand charge transfer (MLCT) bands were seen to exhibit remarkable π-π* character, demonstrated by the strong dependence of the absorptions on the donor/acceptor nature of the carbene carbon substituent. The substituent effect was also found to be related to the equilibrium geometry of the complexes and the occupation of the *p*-atomic orbital of the carbene carbon atom. For example, for styryl-substituted Fischer carbene complexes, π-donor styryl substituents were seen to populate the resonance structure **B** (Scheme 4.1) and therefore shorten the C(carbene)=C bond with concomitant lengthening of the Cr=C bond. Strong acceptor substituents like a cyano group have the opposite effect in the bond distances because the resonance form **B** in Scheme 4.1 cannot be populated. Finally, the ferrocenyl moiety was found to behave as a π-donor group in chromium Fischer carbene complexes. Poorer relations between the bond lengths and the position of absorption maxima of MLCT bands were found than for LF bands. This observation supported the statement that the LF transition displayed higher sensitivity with the π-conjugation compared to the MLCT band.

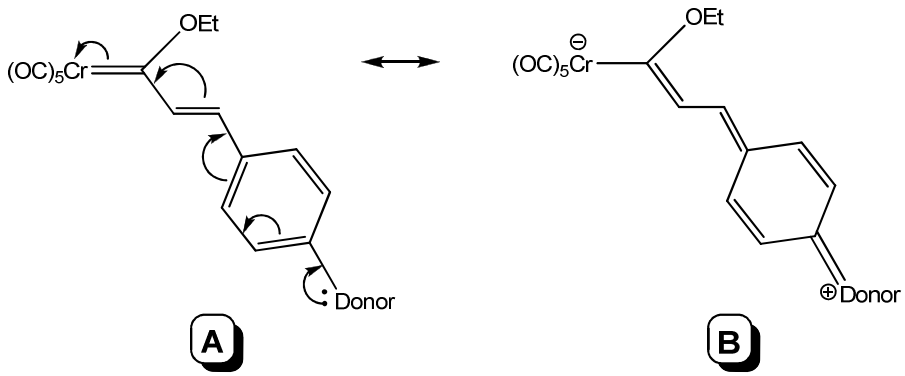

Scheme 4.1

The results of the study changed the interpretation of the UV-vis spectroscopy of Fischer carbene complexes. Earlier results, based on molecular orbital (MO)

calculations,[36] assigned the MLCT band to the promotion of an electron from the nonbonding metal-centred orbital HOMO (highest occupied molecular orbital) to the carbene carbon *p*-orbital-centred LUMO (lowest unoccupied molecular orbital), whereas the LF band was attributed to the more energetic population of the metal-centred LUMO+1. In this study, the TD-DFT calculations assigned the LF band to the HOMO-3 → LUMO transition, and the MLCT was ascribed to the HOMO-1 → LUMO transition.

For the ferrocenyl substituted complexes, slight blue shifts of the MLCT band, and a more pronounced red shift in the LF band correlated with that of the other π-donor substituents. The origin of this donation was found with the help of second-order perturbation theory of the NBO method.[23] A stabilizing two-electron interaction, illustrated in Figure 4.6, between the occupied *d* orbital of the iron atom and the *p* orbital of the carbene carbon atom was found. The associated second-order perturbation energy ($\Delta E^{(2)}$) = -0.60 kcal/mol was determined. This effect was seen as the likely cause for the higher computed *p*-occupation in $[Cr(CO)_5\{C(OEt)Fc\}]$ than in $[Cr(CO)_5\{C(OEt)Ph\}]$.

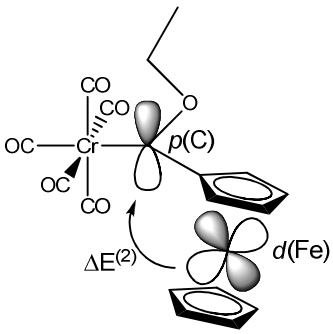

Figure 4.6 Two-electron donation from the iron atom to the carbene carbon atom[25(f)]

[36] (a) Block, T.J.; Fenske, R.F.; Casey, C.P. *J. Am. Chem. Soc.* **1976**, *98*, 441, (b) Nakatsuji, H.; Uskio, J.; Yonezawa, T. *J. Am. Chem. Soc.* **1983**, *105*, 426, (c) Foley, H.C.; Strubinger, L.M.; Targos, T.S.; Geoffroy, G.L. *J. Am. Chem. Soc.* **1983**, *105*, 3064.

4.3 Electrochemical approach

The redox potentials of coordination compounds have been correlated to many other properties along the years, namely the HOMO energy, the gas-phase ionization potential, the ligand field stabilization energy, the energy of charge transfer bands, infrared stretching frequencies, X-ray photoelectron spectroscopy binding energies, NMR parameters and ligand structural parameters, apart from solvent and supporting electrolyte effects.[37] These features are often dependent on the electronic and/or structural properties of the ligands and their coordination metal centers, suggesting that one could define suitable electrochemical parameters, based on the redox potential, for measuring such ligand and metal site properties. The research has often been directed towards the establishment of simple additive ligand effects on the redox potential. This has long been recognized for the series of closely related 18VE octahedral carbonyl/isocyanide complexes $[Mn(CO)_{6-x}(CNR)_x]^+$ (x = 1 – 6).[37(j)] A single electron reversible oxidation associated with an oxidation potential that correlates linearly with the HOMO energy was obtained, where a higher value of the former corresponded to a greater stability of the latter, as expected for an electron removal from the orbital. A linear relationship was developed, containing terms that include a constant that is metal-, solvent- and reference electrode dependent, and the term $[dE°/dx)_L$, i.e. the shift of the oxidation potential per each CO replacement by L as a measure of the effect of the L ligand.

[37] (a) Pombeiro, A.J.L.; Amatore, C. (Eds.) *Trends in Molecular Electrochemistry,* Marcel Dekker/Fontis Media, New York/Lausanne, **2004**, (b) Pombeiro, A.J.L.; McCleverty, J. (Eds.) *Molecular Electrochemistry of Inorganic, Bioinorganic and Organometallic Compounds,* NATO ASI Series, Kluwer, Dordrecht, **1993**, (c) Zanello, P. *Inorganic Electrochemistry: Theory, Practice and Application,* Royal Society of Chemistry, Cambridge, **2003**, (d) Astruc, D. *Electron Transfer and Radical Processes in Transition Metal Chemistry,* VCH, New York, **1995**, (e) Pombeiro, A.J.L. *New J. Chem.* **1997**, *21*, 649, (f) Pombeiro, A.J.L. *Portugaliae Electrochim. Acta* **1983**, *1*, 19, (g) Silva, M.E.N.P.R.A.; Pombeiro, A.J.L.; Fraústo da Silva, J.J.R.; Herrmann, R.; Deus, M.; Bozak, R.E. *J. Organomet. Chem.* **1994**, *480*, 81, (h) Silva, M.E.N.P.R.A.; Pombeiro, A.J.L.; Fraústo da Silva, J.J.R.; Herrmann, R.; Deus, M.; Castilho, T.J.; Silva, M.F.C.G. *J. Organomet. Chem.* **1991**, *421*, 75, (i) Vlcëk, A. *Chemtracts – Inorg. Chem.* **1993**, *5*, 1, (j) Sarapu, A.C.; Fenske, R.F. *Inorg. Chem.* **1975**, *14*, 247, (k) Pickett, C.J.; Pletcher, D. *J. Organomet. Chem.* **1975**, *102*, 327.

Using this approach of the concept that electrochemical potentials are additive with respect to ligand substitution for substituted metal carbonyls as a common basis, electrochemical parameters were defined: the Pickett ligand parameter P_L[37(k), 38] and the Lever ligand parameter E_L.[39] Pickett's and Lever's models of systematic approach have been applied to numerous ligands with electron donor and π-electron acceptor characters, binding various types of metal centers. Pombeiro extended this study to report the estimated electrochemical parameters for carbyne, carbene, vinylidene, allenylidene and alkynyl ligands from the reported values of the redox potentials of their complexes found in the literature.[40] It was found that the net electron acceptance of Group VI transition metal Fischer carbene complexes were sensitive to the nature of the groups attached to the carbene carbon, as a wide range of estimated P_L and E_L values were obtained. The strongest π-electron acceptors, namely diphenyl carbene,[41] displayed an extended conjugated π-system.

4.3.1 Anodic electrochemical behaviour of Fischer carbene complexes

The ferrocenyl carbene complexes[42] with the central metals $M(CO)_5$ (M = Cr, W), systematically exhibit lower oxidation potentials than the related carbene complexes with an alkyl or aryl group instead of ferrocenyl. This behaviour, observed for ferrocenyl alkoxycarbenes, aminocarbenes and anionic oxocarbenes, suggests that the ferrocenyl carbenes are stronger electron donors that the corresponding alkyl or aryl carbenes, on account of an effective π-electron donor ability as ferrocenyl moieties have the known ability to enter

[38] Chatt, J.; Kan, C.T.; Leigh, G.J.; Pickett, C.J.; Stanley, D.R. *J. Chem. Soc., Dalton Trans.* **1980**, 2052.
[39] (a) Lever, A.B.P. *Inorg. Chem.* **1990**, *29*, 1271, (b) Lever, A.B.P. *Inorg. Chem.* **1991**, *30,* 1980.
[40] Pombeiro, A.J.L. *J. Organomet. Chem.* **2005**, *690*, 6021.
[41] Guedes da Silva, M.F.C.; Lemos, M.A.N.D.A.; Fraústo da Silva, J.J.R.; Pombeiro, A.J.L.; Pellinghelli, M.A.; Tiripicchio, A. *J. Chem. Soc., Dalton Trans.* **2000**, 373.
[42] Lloyd, M.K.; McCleverty, J.A.; Orchard, D.G.; Connor, J.A.; Hall, M.B.; Hillier, I.H.; Jones, E.M.; McEwen, G.K. *J. Chem. Soc., Dalton Trans.* **1973**, 1743.

into conjugation with a neighbouring centre by π-donation.[37(g), 43] However, Pombeiro cautioned that the electrochemical parameters of $[M(CO)_5\{C(X)Fc\}]$ complexes encompass both the redox M^0 and Fe^{2+} centers, as the HOMO is not simply localized at the former.[40]

Another electrochemical study of ferrocenyl carbenes involved the reaction of ferrocene amides $(Ph_2P)Fc'C(O)NR_2$ (complex **I** as shown in Scheme 4.2) with $[Cr(CO)_5]^{2-}$ in the presence of Me_3SiCl to give the respective P-chelated carbene complex $[Cr(CO)_4\{(Ph_2P)Fc'C(NR_2)\text{-}\mu_2\text{-}C,P\}]$ (**II**) and a phosphine complex (**III**).[44]

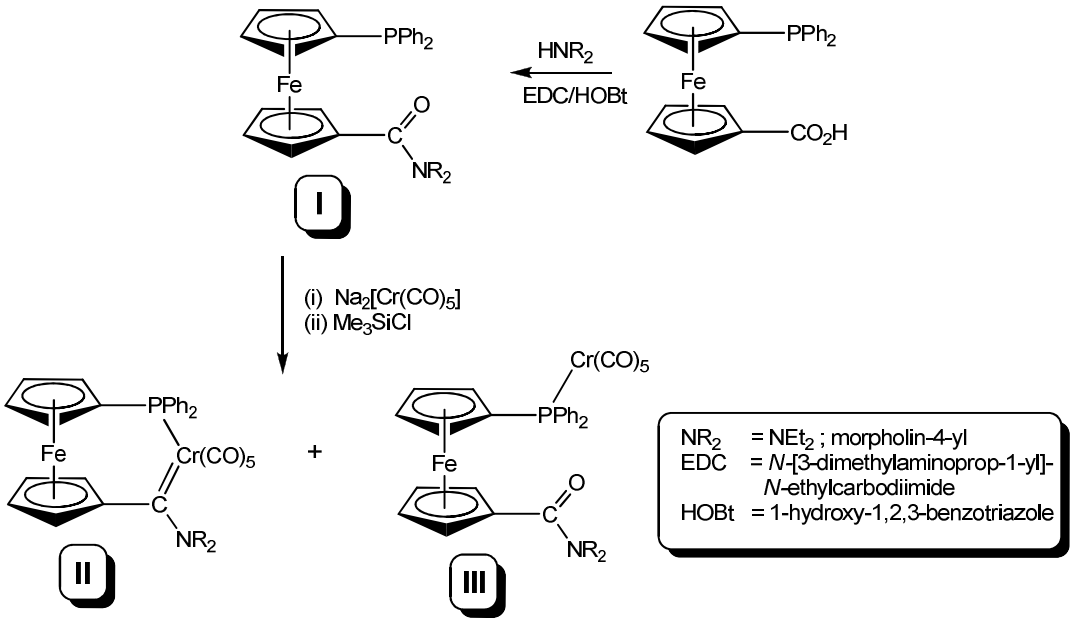

Scheme 4.2

An electrochemical analysis showed that where compounds **I** and **III** behave as a simple ferrocene system (**I**) and two localized redox systems (**III**) (ferrocene and chromium), respectively, carbene **II** is an electronically delocalized system, where the redox change probably occurs in the whole molecule.

[43] Gubin, S.P.; Lubovich, A.A. *J. Organomet. Chem.* **1970**, *22*, 183.
[44] Meca, L.; Dvořák, D.; Ludvík, J.; Císařová, I.; Stěpnička, P. *Organometallics* **2004**, *23*, 2541.

Unlike the $[Cr(CO)_5\{C(Y)Fc\}]$ carbene complexes, which display a single one-electron wave ascribed to the removal of an electron from a molecular orbital which encompasses both metal centres,[42] the type **II** carbene complexes exhibit two one-electron redox processes. The first oxidation is reversible, shifted to markedly lower potentials than in the other compounds. The negative shift of the first oxidation wave in **II** was accounted for by the cooperative influence of the higher electron donating ability of NR_2 as compared to the OR group, and an electron density increase resulting from a replacement of one CO ligand with a phosphine, which makes the oxidation easier. This indicated that carbenes **II** are an example of the cooperative effect of the metal centre, enhanced by a conjugated bridge.

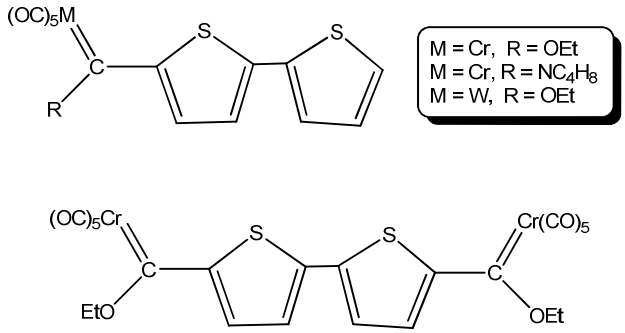

Scheme 4.3

Limberg *et al.* investigated the electrochemical behaviour of mono- and biscarbene complexes of chromium and tungsten by cyclic voltammetry (CV) and controlled potential electrolysis (CPE).[45] The complexes, illustrated in Scheme 4.3, all showed a single anodic wave. For the chromium compounds, this wave presented a partially reversible character, whereas the oxidation wave of the tungsten compound was irreversible.

The cyclic voltammograms displayed several cathodic waves. For the ethoxy substituted complexes, the first reduction waves were reversible, and found in

[45] Limberg, A.; Lemos, M.A.N.D.A.; Pombeiro, A.J.C.; Maiorana, S.; Papagni, A.; Licandro, E. *Portugaliae Electrochim. Acta* **1995**, *13*, 319.

the range -0.70 V to -1.02 V. However, the aminocarbene complex showed an irreversible cathodic wave at a remarkably more negative potential (-1.68 V). This large potential shift was seen as being due to the electron donating character of the amino group, and a possible indication that the energy of the LUMO is much influenced by carbene substituents, as expected for a significant contribution of the carbene carbon to that orbital as observed for related carbene complexes.[46]

Expanding on the cyclic voltammetry study of Group VI transition metal Fischer carbene complexes and focusing on the modulating effects of both the carbene metal and substituent, the group of Maiorana studied complexes of the type $[M(CO)_5\{C(XR)R'\}]$ (M = Cr; Mo; W and X = O; S; NR'').[47] It was found that the first oxidation step of the chromium compounds were significantly easier that that of the tungsten counterparts. This was correlated to the first ionization potentials of the two metals in gas phase (652.9 $kL.mol^{-1}$ for Cr and 770 $kJ.mol^{-1}$ for W),[48] indicating that the oxidation step is centred on the carbene metal.
The tungsten complexes featured chemically irreversible oxidation peaks, while the chemically reversible and monoelectronic peak of the chromium complexes implies that a chemically stable product forms. The potentials were also found to be widely modulable by changing both the XR and R' substituents.

4.3.2 Cathodic behaviour of Fischer carbene complexes

Fischer carbene complexes contain the electron withdrawing $M(CO)_5$-moieties, which make the carbene carbon atoms very electrophilic; hence, the carbene carbons are good electron acceptors. From DFT calculations, it can be seen that the LUMO is centred on the carbene carbon while the HOMO is metal-centred.[49] Therefore, the capture of one electron should succeed in a much more localized

[46] Casey, C.P.; Albin, L.D.; Saeman, M.C.; Evans, D.H. *J. Organomet. Chem.* **1978**, *155*, C37.
[47] Baldoli, Cl; Cerea, P.; Falciola, L.; Giannini, C.; Licandro, E.; Maiorana, S. ; Mussini, P. ; Perdicchia, D. *J. Organomet. Chem.* **2005**, *690*, 5777.
[48] Center for X-ray Optics and Advanced Light Source, X-ray Data Booklet **2001**, Lawrence Berkeley National Laboratory, University of California.
[49] Sierra, M.A.; Gòmez-Gallego, M.; Martínez-Álvarez, R. *Chem. Eur. J.* **2007**, *13*, 736.

site of the molecule, while the negative charge will be centred on the metal, and stabilized species may arise from the capture of one electron.

The single electron transfer (SET) of Group VI Fischer carbene complexes was investigated by chemical reagents (such as C_8K and SmI_2), as well as electrospray ionization (ESI) by Sierra *et al.*[49] The results obtained indicate that depending on the stability of the radical ion formed, the electrophile present in the reaction medium and the nature of the metal, different reaction products could be observed, from CO_2 trapping, to addition to electron poor olefins, CO insertions and dimerizations.

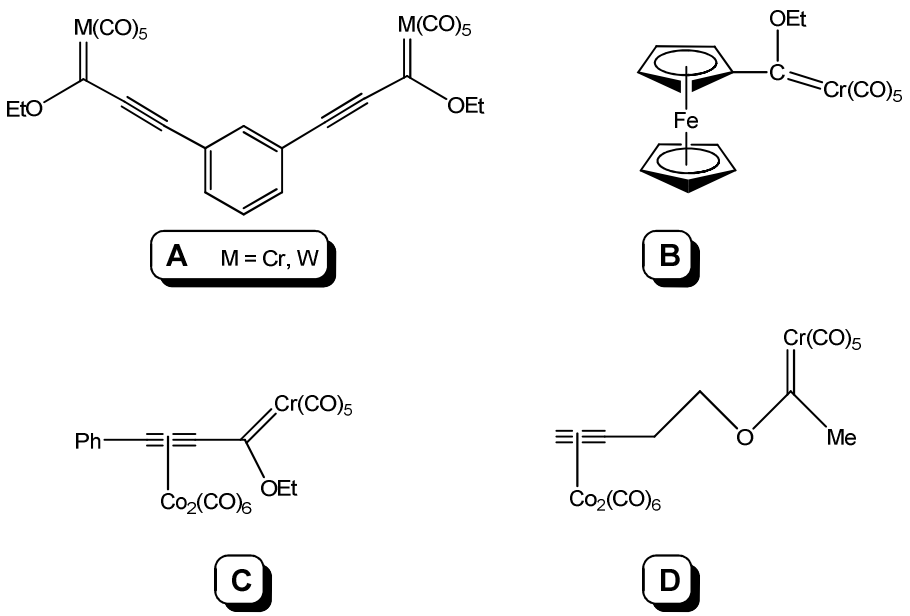

Scheme 4.4

The ESI-ET behaviour of metal carbene complexes could also be influenced by the presence of additional metal centres. Thus, the presence of two nonconjugated metal carbene moieties in homo- and heterobimetallic biscarbene complexes (**A** in Scheme 4.4) did not alter the general reactivity, and behaved in a similar fashion as the corresponding monocarbene complex $[Cr(CO)_5\{C(OEt)C{\equiv}CPh\}]$ in the presence of electron carrier additives such as tetrathiafulvalene (TTF) or hydroquinone (HQ). In electrochemical studies, the

biscarbene complexes have also been found to behave as two independent monocarbene entities.[50]

The presence of a conjugated ferrocene moiety in the structure of the Fischer carbene comlexes, however, has a noticeable effect in the course of the ESI ionization.

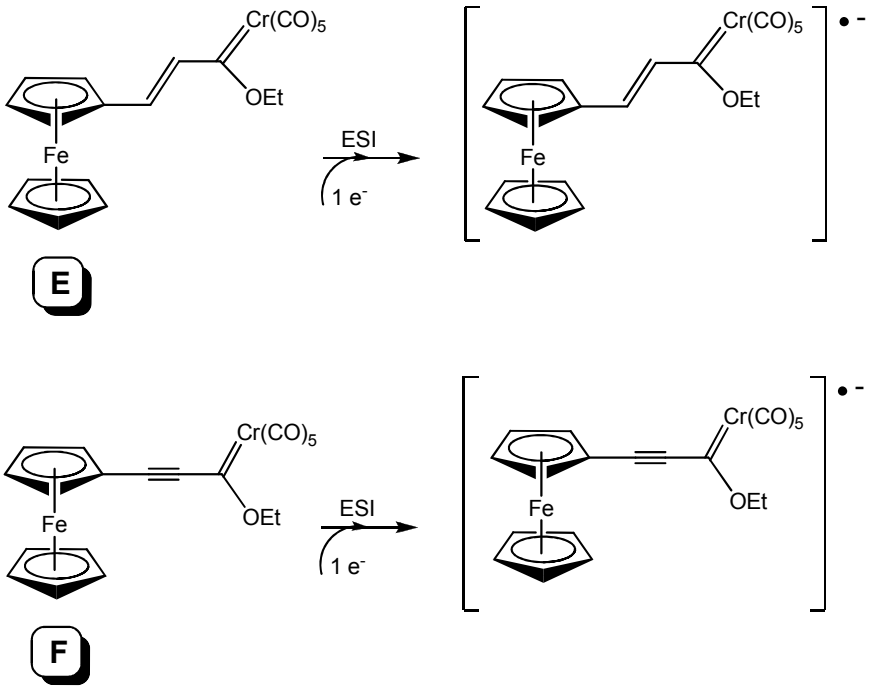

Figure 4.7 The ferrocenyl moiety acting as internal electron carrier in conjugated bimetallic carbene complexes

Ferrocenyl complexes **E** and **F** in Figure 4.7, ionize under ESI conditions even in the absence of the additives TTF and HQ, leading to radical anions. The experimental results could be understood considering the push-pull nature of these complexes. The ferrocenyl moiety is an electron donor and the $Cr(CO)_5$-group behaves like a large electron depleted group, since the five CO ligands are strong π-acceptors. Ferrocene can therefore be considered as an internal electron carrier that facilitates the direct formation of the carbene radical anion.

[50] Martínez-Álvarez, R.; Gòmez-Gallego, M.; Fernández, I.; Mancheño, M.J.; Sierra, M.A. *Organometallics* **2004**, *23*, 4647.

However, for complex **B** in Scheme 4.4, there is no π-tether linking the iron nucleus to the chromium, and no direct electrospray ionization could take place.

The presence of cobalt clusters exercised a radical effect in the ESI of the Group VI Fischer carbene complexes. When the $Co_2(CO)_6$-moiety was included in the structure of the complexes (**C** and **D** in Scheme 4.4), the electron transfer process from the additives was hampered. The ablility of $[Co_2(CO)_8]$ towards reduction is well known[51] and therefore the bimetallic cluster is seen as behaving as an electron sink inhibiting the ionization process.

4.4 Results and discussion

4.4.1 Focus of this study

The paper published by Cundari and Gordon[52] focused on the effect of ligand and substituent modification on the transition metal-alkylidene bond. They found that the intrinsic nature of the metal-carbon double bond could typically be changed within limits by modification of the electronegativities of the two carbene ligand substituents. Significant changes could be effected in three other ways: (i) variation of the central metal, (ii) use of π-donor substituents at the carbene group, and (iii) introduction of highly electropositive substituents like Li.

In this study, the aim was to investigate the effect of substituents on the carbene ligand of Group VI transition metal complexes of the type $[M(CO)_5\{C(OR)Y\}]$. The substituents included in this study ranged from the usual organic substituents (R = Et and Y = 2-benzothienyl or 2-thienyl); or metal-containing fragments that could either act as π-donors (Y = Fc), an electron sink (Y = $[Cr(CO)_3(2\text{-}\eta^6\text{-benzo[}b\text{]thienyl})]$ or $[Cr(CO)_3(\eta^6\text{-phenyl})]$) where a $Cr(CO)_3$-moiety is π-bonded to a (hetero)arene ring, or an electropositive titanoxy group (R =

[51] (a) Sweany, R.L. *Comprehensive Organometallic Chemistry II,* (Eds. Abel, E.W.; Stone, F.G.; Wilkinson, G.), Pergamon, Oxford, **1995**, *8*, (b) Gibson, D.H.; Ahmed, F.U.; Philips, K.R. *J. Organomet. Chem.* **1981**, *218*, 325.
[52] Cundari, T.R.; Gordon, M.S. *J. Am. Chem. Soc.* **1992**, *114*, 539.

$TiCp_2Cl$), as listed in Figure 4.8, in order to effect marked modulation of the carbene ligands, as stipulated by Cundari and Gordon.[52]

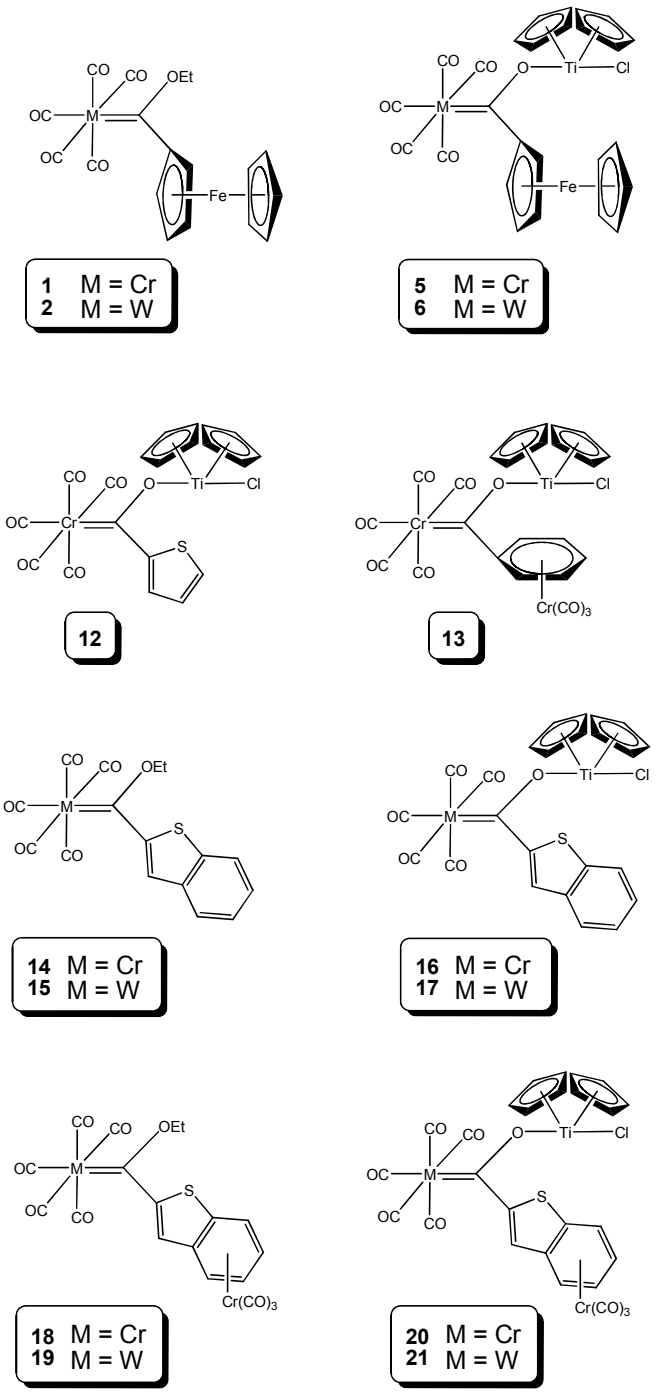

Figure 4.8 Monocarbene complexes studied by theoretical and electrochemical means

The synthesis and X-ray structural elucidation of the benzothienyl carbene complexes **14** – **21** have been previously published by our research group,[53] but were included for purposes of comparison in this study. Both theoretical and electrochemical methods were employed during this study. The possibility of using DFT calculations as a viable tool for pre-evaluation of cluster carbene complexes was also investigated.

4.5 Theoretical investigation of substituent effect

4.5.1 Computational details

The calculations reported in this chapter were obtained with the GAUSSIAN 03 suite of programmes.[54] Each complex was treated as an open-shell system using spin restricted DFT wavefunctions (RB3LYP)[55] i.e. the Becke three-parameter exchange functional in combination with the LYP correlation functional of Lee, Yang and Parr, with effective core potentials basis set LANL2DZ for the metal atoms. This method was specifically chosen as it allows increased accuracy of the model, with a small increase in the computation time; the increased accuracy arising from the inclusion of electron correlation effects where electrons interact with other electrons, not just an averaged electron cloud.[17] This is a quantum mechanical model, making use of the wavefunction of

[53] (a) Bezuidenhout, D.I.; van der Watt, E.; Liles, D.C.; Landman, M.; Lotz, S. *Organometallics* **2008**, *27*, 2447, (b) Van der Watt, E. *Fischer carbene complexes with metal-containing substituents,* MSc. Dissertation, University of Pretoria, Pretoria, **2006**.

[54] Frisch, M.J.; Trucks, G.W.; Schlegel, H.B.; Scuseria, G.E.; Robb, M.A.; Cheeseman, J.R.; Montgomery Jr, J.A.; Vreven, T.; Kudin, K.N.; Burant, J.C.; Millam, J.M.; Iyengar, S.S.; Tomasi, J.; Barone, V.; Mennucci, B.; Cossi, M.; Scalmani, G.; Rega, N.; Petersson, G.A.; Nakatsuji, H.; Hada, M.; Ehara, M.; Toyota, K.; Fukuda, R.; Hasegawa, J.; Ishida, M.; Nakajima, T.; Honda, Y.; Kitao, O.; Nakai, H.; Klene, M.; Li, X.; Knox, J.E.; Hratchian, H.P.; Cross, J.B.; Bakken, V.; Adamo, C.; Jaramillo, J.; Gomperts, R.; Stratmann, R.E.; Yazyev, O.; Austin, A.J.; Cammi, R.; Pomelli, C.; Ochterski, J.W.; Ayala, P.Y.; Morokuma, K.; Voth, G.A.; Salvador, P.; Dannenberg, J.J.; Zakrzewski, V.; Dapprich, S.; Daniels, A.D.; Strain, M.C.; Farkas, O.; Malick, D.K.; Rabuck, A.D.; Raghavachari, K.; Foresman, J.B.; Ortiz, J.V.; Cui, Q.; Baboul, A.G.; Clifford, S.; Cioslowski, J.; Stefanov, B.B.; Liu, G.; Liashenko, A.; Piskorz, P.; Komaromi, I.; Martin, R.L.; Fox, D.J.; Keith, T.; Al-Laham, M.A.; Peng, C.Y.; Nanayakkara, A.; Challacombe, M.; Gill, P.M.W.; Johnson, B.; Chen, W.; Wong, M.W.; Gonzalez, C.; Pople, J.A. *Gaussian 03*, revision C.02; Gaussian, Inc.: Wallingford, CT, **2004**.

[55] (a) Becke, A.D. *J. Chem. Phys.* **1993**, *98*, 5648, (b) Lee, C.; Yang, W.; Parr, R.G. *Phys. Rev. B* **1998**, *37*, 785, (c) Vosko, S.H.; Wilk, L.; Nusair, M. *Can. J. Phys.* **1980**, *58*, 1200.

the electrons, rather than the Newtonian-like molecular mechanics. The basis set LANL2DZ was chosen as it includes relativistic effects, which become important for the heavy atoms like W in the complexes. No symmetry constraints were applied and only the default convergence criteria were used during the geometric optimizations. The complexes were all modelled in the singlet spin state with S = ½ and the optimized structures were confirmed to be minima energy conformations as the vibrational frequency analysis[56] yielded no imaginary frequencies.

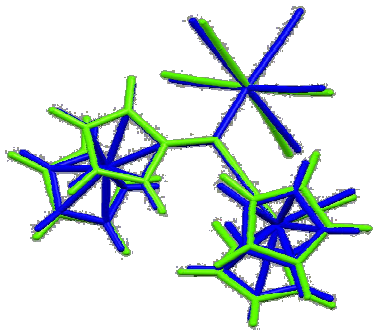

Figure 4.9 Representative overlay of experimental crystal structure and DFT optimised structure of complex **5**

The accuracy of the computational method was evaluated by comparing the root-mean-square deviations (RMSD's) between the optimized molecular structure and the crystal structure using the non-hydrogen atoms in the molecule. RMSD values were calculated using the 'RMS Compare Structures' utility in CHEMCRAFT Version 1.5.[57] Good agreement between experimental and theoretical structures was obtained as illustrated in Figure 4.9, and reflected by root-mean-square deviation (RMSD's) values in the range of 0.10 – 0.16 Å for the chromium complexes, and 0.06 – 0.19 Å for the tungsten complexes.

[56] McIver, J.W.; Komornicki, A.K. *J. Am. Chem. Soc.* **1972**, *94,* 2625.
[57] Zhurko, G.A.; Zhurko, D.A. *Chemcraft*, Version 1.5 (build 282), **2007**.

4.5.2 Theoretical results

Initially it was attempted to correlate the donor properties of the various carbene ligands in the complexes listed in Figure 4.8, with both the C≡O stretching frequencies and bond lengths with the aid of DFT calculations, as illustrated by Gusev.[58] The A_1^1 band, the mode associated with the stretching of the C-O bond *trans* to the carbene ligand was chosen as probe, as it is expected to be most affected by the electronic environment.

It is well known that (i) the assumption of an harmonic force field, (ii) the neglect or inadequate treatment of electron correlation effects and (iii) basis set deficiencies are sources of error in quantum mechanically computed vibrational frequencies.[59] Therefore it is common to multiply computed vibrational frequencies by a scale factor developed to minimize the RMS error from experiment. For organometallic complexes, it has been found that almost invariably, computed frequencies are greater than experiment.[60] For organometallic complexes, the CO vibrational frequencies determined at the B3LYP level with the relativistic core potential LANL2DZ, delivered reliable results from an optimized scale factor of 0.9521. The results obtained from this study gave a reasonable estimation of the carbonyl IR frequencies when compared to the experimental data of the solution IR spectra (reported in Chapter 2, as well as in previous studies[53] for the complexes **14** – **21**). However, the modelled data displayed consistent underestimations of the A_1^1 band frequencies calculated, the absolute deviations ranging from 10 – 60 cm^{-1}. The experimental solution IR data were therefore corrected by applying a scale factor of 1.02 to the modelled data. As the experimental data includes solution IR data recorded in either solvent hexane or dichloromethane, the scaled frequencies calculated by DFT methods were used to eliminate solvent effects.

[58] Gusev, D.G.; *Organometallics* **2009**, *28*, 763.
[59] Scott, A.P.; Radom, L. *J. Phys. Chem.* **1996**, *100*, 16502.
[60] Yu, L.; Srinivas, G.N.; Schwartz, M. *J. Mol. Struct. (Theochem)* **2003**, *625*, 215, and references therein.

The calculated frequencies for the A_1^1 band are tabulated in Tables 4.1 and 4.2 in order of decreasing wavenumbers, and should provide an indication of the π-acceptor ability of the relevant carbene ligand: the lower the wavenumber of the ν(CO), the weaker the *trans*-C-O bond, implying increased bond strength of the *trans*-OC-M bond and resultant decreased bond strength of the M=C(carbene). Tables 4.1 and 4.2 therefore also include the experimental bond lengths of the crystal structures. Not only the M=C(carbene) and *trans*-OC-M bond lengths were included, but also the *trans*-C-O, the C(carbene)-O and the C(carbene)-C((hetero)arene substituent) in order to determine if a trend could be established towards substituent involvement towards carbene stabilization.

For the sake of clarity, each complex [$M(CO)_5${C(OR)(hetero)aryl}] will be denoted by its central metal, eg. $Cr(CO)_5$-group represented by Cr; the (hetero)aryl ring substuent indicated as BT for 2-benzothienyl, T = 2-thienyl, Fc = ferrocenyl, BTCr = [$Cr(CO)_3(\eta^6$-2-benzo[*b*]thienyl)] and PhCr = [$Cr(CO)_3(\eta^6$-phenyl)], and R = Et (ethyl) or Ti (titanocene chloride). Therefore, complex **5** [$Cr(CO)_5${C(OTiCp_2Cl)Fc}] for example, will be represented by the abbreviation CrFcTi, and so on. The tables are colour coded, with red indicating the greatest value, and the smallest value coloured blue.

In general, the A_1^1 frequencies seem to correlate well with the M=C(carbene) bond lengths, for both the chromium and tungsten complexes, with the shortest bond distances obtained for the MBTCrET complexes **18** and **19**, respectively, corresponding to the highest ν(CO) wavenumbers. The weakest M=C bonds are the MFcTi, MFcET and MBTTi complexes (**5** and **6**; **1** and **2**; **16** and **17** respectively, M = Cr or W), which correspond to the lowest ν(CO) wavenumbers.

Table 4.1 Scaled, calculated A_1^1 frequencies (cm^{-1}) and associated experimental bond lengths (Å) of selected chromium carbene complexes

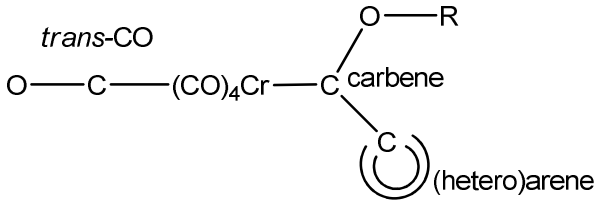

Complex	A_1^1 ν(CO)*	Bond lengths				
		trans-C-O	Cr-CO_{trans}	Cr-$C_{carbene}$	$C_{carbene}$-O	$C_{carbene}$-$C_{(hetero)arene}$
18 CrBTCrEt	1971	1.139(3)	1.884(3)	2.050(2)	1.324(3)	1.472(3)
13 CrPhCrTi	1968	1.146(5)	1.879(4)	2.067(3)	1.287(4)	1.513(5)
20 CrBTCrTi	1967	1.159(7)	1.859(6)	2.077(4)	1.285(5)	1.463(6)
14 CrBTEt	1964	1.143(3)	1.875(3)	2.067(3)	1.319(3)	1.462(3)
12 CrTTi	1961	1.150(3)	1.866(3)	2.081(2)	1.283(2)	1.442(5)
16 CrBTTi	1960	1.073(5)	1.926(9)	2.104(7)	1.275(9)	1.461(13)
1 CrFcEt	1959	1.135(3)	1.876(3)	2.084(2)	1.317(2)	1.452(3)
5 CrFcTi	1957	1.151(6)	1.863(5)	2.090(4)	1.286(5)	1.472(6)

* Corrected by a scale factor of 1.02

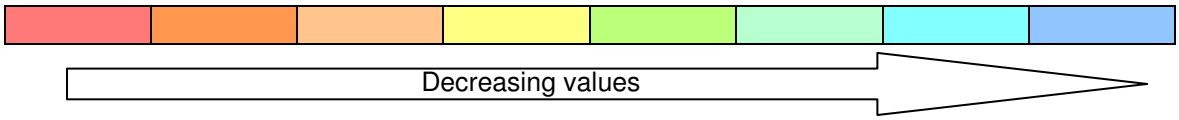

Table 4.2 Scaled, calculated A_1^1 frequencies (cm^{-1}) and associated experimental bond lengths (Å) of selected tungsten carbene complexes

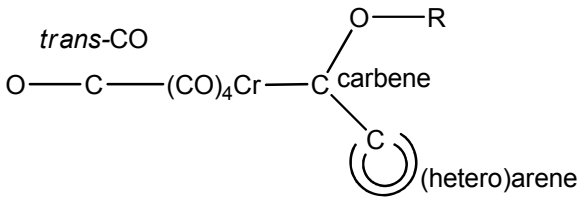

Complex	A_1^1 ν(CO)*	Bond lengths				
		trans-C-O	W-CO_{trans}	W-$C_{carbene}$	$C_{carbene}$-O	$C_{carbene}$-$C_{(hetero)arene}$
19 WBTCrEt	1951	1.147(9)	2.011(7)	2.179(7)	1.318(8)	1.471(8)
21 WBTCrTi	1946	1.151(7)	2.000(6)	2.207(4)	1.280(5)	1.461(6)
15 WBTEt	1945	1.139(7)	2.018(6)	2.201(5)	1.315(6)	1.468(7)
2 WFcEt	1941	1.136(5)	2.018(5)	2.215(4)	1.335(5)	1.466(6)
17 WBTTi	1940	1.149(5)	2.007(4)	2.211(4)	1.279(4)	1.474(5)
6 WFcTi	1938	1.155(14)	2.008(13)	2.253(9)	1.273(11)	1.465(15)

* Corrected by a scale factor of 1.02

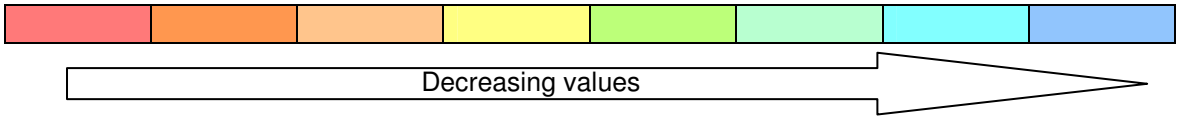

For both cases Cr and W as central method, a marked increase in C(carbene)-O bond length is observed for the ethoxycarbenes compared to the titanoxycarbene complexes. However, from the data in Table 4.2 a further distinction can be made: for either ethoxy- or titanoxycarbenes, the C(carbene)-

O bond distances increase in the substituent order Fc < BT < BTCr. Assuming that greater *O*-heteroatom stabilization towards the carbene carbon is necessary for ferrocenyl *vs* benzothienyl substituents is however not justified, as the C(carbene)-C(ring) bond lengths should then follow the inverse trend to demonstrate ring-involvement towards stabilization. For example, CrPhCrTi (**13**) exhibits long C(carbene)-O and C(carbene)-C(ring) bond distances, and a short Cr=C(carbene) bond length corresponding to a weak Cr-$(CO)_{trans}$ bond and high A_1' frequency. However, CrBTTi (**16**) shows the weakest Cr=C(carbene) bond, as well as the weakest Cr-$(CO)_{trans}$ bond. The shortest C(carbene)-O bond is also observed for this complex, which would seem to indicate most stabilization from the acyl-like titanoxy group. However, steric factors were not included in these arguments, which complicates identification of a clear trend from this data.

4.5.3 Vibrational spectroscopy results

To exclude solvent effects, solid, crystalline samples of complexes **5** and **6** (MFcTi); **18** and **19** (MBTCrEt); and **20** and **21** (MBTCrTi) (M = Cr, W) were obtained and solid state infrared spectra measured. The Raman spectra of the same complexes were also measured, using the 647.1 nm (red) line of a Krypton-ion laser. The IR data displayed clearly resolved spectra, with the expected localized C_{4v} pattern[61] of the IR-active A_1^2, A_1^1 and E-modes. Although all four modes (A_1^2, A_1^1, B_1 and E) are Raman-active, only the A_1^1 and A_1^2 bands were observed in the Raman spectra. In addition, the A_1^1 band (specifically, the vibrational ν(*trans*-C-O) frequency of interest) was not observed in the presence of titanoxycarbene substituents due to distortional effects, as illustrated in Figure 4.10. From the crystal structures of these complexes, it can be seen that the Cl-atom of the titanoxy substituent protrudes in between two *cis*-CO ligands (Figure 4.11). This distortion of the C_{4v} symmetry can lead to loss or reduction of symmetry, resulting in either C_s or C_{2v} symmetry which explains the disappearance of some Raman active vibrational modes.

[61] Adams, D.M. *Metal-Ligand and Related Vibrations,* Edward Arnold Publishers Ltd., London, **1967**, 98.

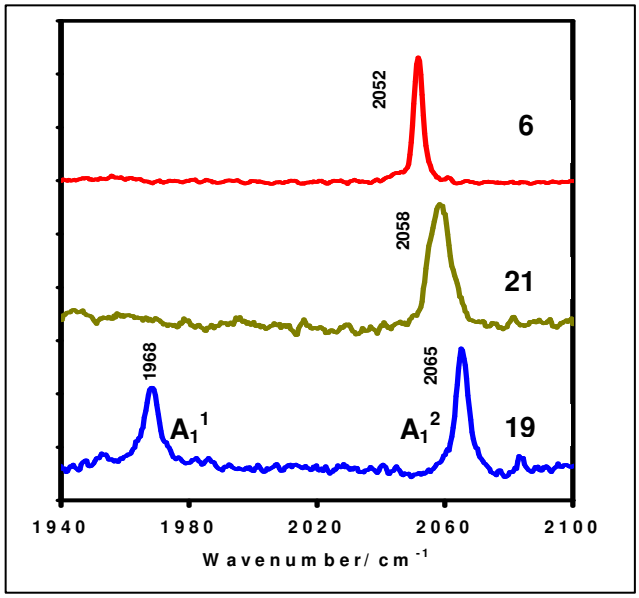

Figure 4.10 ν(CO) region of the Raman spectra of complexes **6, 19** and **21,** showing the disappearance of the A_1^1 band due to distortion effect of –$TiCp_2Cl$ substituent

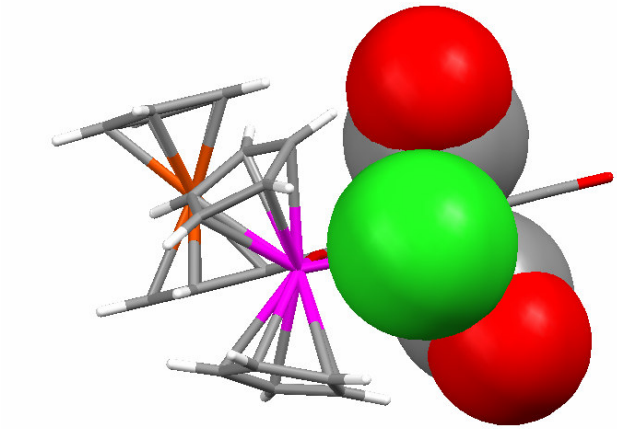

Figure 4.11 Space-filled representation of the Cl-atom (green) protruding between two *cis*-CO ligands of complex **6**

The above observation meant that the A_1^1 band could therefore not be used as a probe for substituent effect. Not only is the A_1^1 band absent in the Raman spectra of the titanoxy complexes, but DFT calculations also indicated significant contribution from the π-bonded $Cr(CO)_3$-fragment, where present. Therefore, other substituent influenced vibrational bands had to be employed in this investigation.

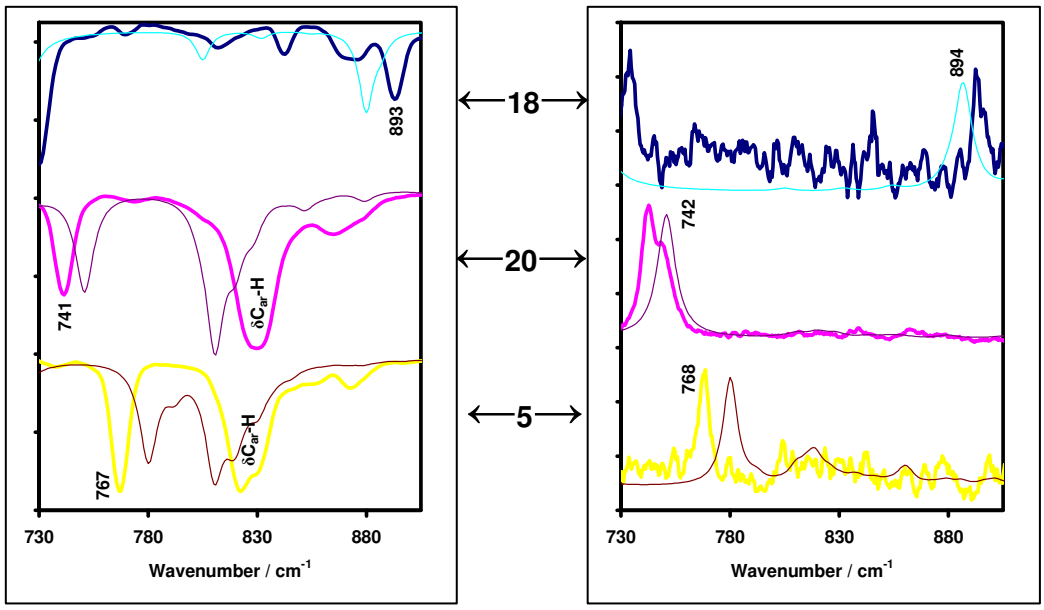

Figure 4.12 Comparative experimental (bold) and unscaled calculated (thin line) IR (left) and Raman (right) spectra of the $\delta CC_{carbene}O$ scissor mode for the chromium complexes

For $M(CO)_5L$ molecules, three IR active $\nu(M\text{-}C_{carbonyl})$ vibrations occur (2 A_1 + E) in the far-infrared region, usually in the range of 380 – 500 cm^{-1}.[62] These metal-carbon stretching vibrations fall within range of the chromium tricarbonyl-fragment $M\text{-}C_{carbonyl}$ and other M-L vibrations, eg. Ti-Cl etc. DFT calculations were therefore employed to assist in the assignment of a $M\text{-}C_{carbene}$ stretching frequency. As far as could be ascertained, no such vibrational bands have been reported to date. However, the modelled data indicated that no pure $\nu(M\text{-}C_{carbene})$

[62] Darensbourg, M.Y.; Darensbourg, D.J. *Inorg. Chem.* **1970**, *9*, 32.

mode exists. Instead, a bending vibration or scissor mode could be identified from the calculations. A representative overlay of the measured experimental IR and Raman spectra and the calculated spectra used for assignment is demonstrated in Figure 4.12. The IR spectra illustrated in Figure 4.12 also display the ring-C-H deformation ($\delta C_{aromatic}$-H) modes. The $\delta(CC_{carbene}O)$ scissor mode consists of a stretching vibration of the carbene carbon atom towards the central metal atom, with contribution from the carbene carbon substituents, as depicted in Figure 4.13. This carbene ligand associated band was observed at higher wavenumbers than the $\nu(M\text{-}C_{carbonyl})$ bands in both the solid state IR and Raman spectra, and assignment of the scissor mode-related band, as well as the other substituent-influenced band, the A_1^1 $\nu(CO)$ mode, are done in Table 4.3.

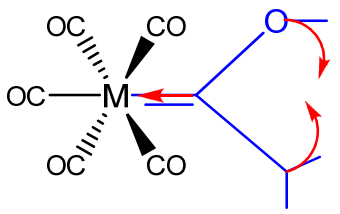

Figure 4.13 A schematic representation of the $\delta CC_{carbene}O$ scissor mode

Table 4.3 Experimental IR and Raman data of substituent influenced vibrational bands (cm^{-1})

Assignment	**18** CrBTCrEt		**20** CrBTCrTi		**5** CrFcTi	
	IR	Raman	IR	Raman	IR	Raman
$\nu(CO)$ A_1^1	1963	1968	1934	-	1921	-
$\delta CC_{carbene}O$	893	894	741	742	767	768
Assignment	**19** WBTCrET		**21** WBTCrTi		**6** WFcTi	
	IR	Raman	IR	Raman	IR	Raman
$\nu(CO)$ A_1^1	1960	1968	1913	-	1928	-
$\delta CC_{carbene}O$	895	895	746	748	774	774

The carbene ligand associated δCCO band displayed the highest energy for the η^6-2-benzo[*b*]thienyl chromium tricarbonyl ethoxy-substituted carbene complexes, corresponding to the shortest M=C(carbene) bond lengths tabulated in Tables 4.1 and 4.2. This supports the supposition that greater backdonation from the metal is necessary for a ring substituent π-bonded to a $Cr(CO)_3$-fragment that acts as an electron sink, minimizing ring-involvement towards carbene stabilization. The acyl character of the carbene oxygen atom of the titanoxy substituents (as discussed in previous chapters) could also be assumed to require less metal donation to the carbene carbon *p* orbital as it is a better π-donor, compared to that of the ethoxycarbenes. However, when the titanoxy substituent is kept constant and the effect of the η^6-2-benzo[*b*]thienyl chromium tricarbonyl *vs* the ferrocenyl substituent is compared, lower δCCO frequencies are obtained for the [$Cr(CO)_3$(η^6-2-benzo[*b*]thienyl)]-complexes even though Fc is the better π-donor. This could be ascribed to the greater bulk of the aforementioned substituent compared to that of Fc, contributing to the moment of inertia of the scissor mode. This result therefore does not preclude the spectroscopic data as a viable tool for substituent effect investigation, but both steric and electronic effects should be taken into account before any conclusions can be drawn. The calculated force constants of the vibrations were also considered, but followed the same order of magnitude trends as the actual vibrational frequencies.

4.5.4 Molecular orbital analysis

Comparison of the charges of the atoms calculated *via* Mulliken population analysis[63] cannot be done by considering the absolute values, as the chromium complexes display negatively charged Cr atoms compared to the positive W atoms. Instead the absolute differences between central metal atom and carbene carbon atom; carbene oxygen and carbene carbon atoms; and carbene

[63] Mulliken, R.S. *J. Chem. Phys.* **1955**, *23*, 1833.

carbon and arene substituent carbon atoms are used in the analysis of the atomic charges. The values are listed in Table 4.4.

Table 4.4 Calculated Mulliken charge differences of relevant atoms in carbene complexes

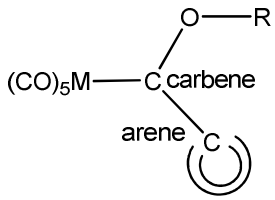

Complex	| Cr – $C_{carbene}$ |	| O – $C_{carbene}$ |	| C_{arene} – $C_{carbene}$ |
1 CrFcEt	0.726	0.496	0.002
5 CrFcTi	0.597	0.720	0.020
12 CrTTi	0.711	0.876	0.544
13 CrPhCrTi	0.581	0.714	0.156
14 CrBTEt	0.846	0.662	0.565
16 CrBTTi	0.688	0.854	0.509
18 CrBTCrEt	0.821	0.641	0.554
20 CrBTCrTi	0.673	0.844	0.638
Complex	| W – $C_{carbene}$ |	| O – $C_{carbene}$ |	| C_{arene} – $C_{carbene}$ |
2 WFcEt	0.592	0.258	0.236
6 WFcTi	0.746	0.507	0.145
15 WBTEt	0.338	0.501	0.423
17 WBTTi	0.549	0.708	0.394
19 WBTCrEt	0.370	0.478	0.424
21 WBTCrTi	0.543	0.698	0.529

The blue and red coded cells in the table indicate heteroatom substituent effect: for ethoxy substituted complexes, a larger charge difference (blue) between the

Cr atom and carbene carbon is observed, as the titanoxy substituent is expected to better stabilize the carbene carbon atom, due to the greater electron density present on the titanoxy-O atom (red) compared to that of the ethoxy-O atom. For the tungsten complexes, the W atom is originally assigned a positive charge in contrast to the negative charge of the Cr atom. The inverse trend observed (blue) therefore indicates agreement of the results obtained for the chromium complexes.

The charge differences between carbene carbon atom and (hetero)arene carbon should indicate to what extent the π-ring is involved towards stabilization of the carbene, as aromaticity is disrupted. In the case of the η^6-phenyl chromium tricarbonyl substituted complex **13** (yellow), the small difference value can be ascribed to the 'electron sink' capability of the $Cr(CO)_3$-fragment, drawing electron density towards itself. For the η^6-2-benzo[*b*]thienyl chromium tricarbonyl complexes, the $Cr(CO)_3$-moiety is not bonded to the thienyl ring which is directly bonded to the carbene carbon atom, and therefore does not display such a marked effect. On the other hand, the small difference values obtained for the ferrocenyl complexes can be explained by the stabilization effect of ferrocenes that takes place through π-delocalization rather than through inductive effects.[64]

The importance of the LUMO of Fischer carbene complexes in the nucleophilic attack of carbene carbons were explained by Block *et al*.[36(a)] Calculated atomic charges indicated that the carbene carbon atom is less positive than the carbonyl carbons, in agreement with the X-ray photoelectron spectroscopic data of Perry.[65] Nevertheless, the carbene carbon was found to be the preferred site for nucleophilic attack and charge did not determine reactivities.
However, frontier orbital control,[66] which emphasizes the importance of a compound's HOMO or LUMO in determining which sites in the molecule will be most susceptible to attack by an electrophile or nucleophile could explain the reactivities. A striking result of the MO calculations on the carbene complexes

[64] Connor, J.A.; Lloyd, J.P. *J. Chem. Soc., Dalton Trans.* **1972**, 1470.
[65] Perry, W.B.; Schaaf, T.F.; Jolly, W.L.; Todd, L.J.; Cronin, D.L. *Inorg. Chem.* **1973**, *13*, 2038.
[66] (a) Fukui, K.; Fujimoto, H. *Bull. Chem. Soc. Jpn.* **1969**, *42*, 3399, (b) Klopman, G.; Hudson, R.F. *Theor. Chim. Acta* **1967**, *8*, 165.

was the marked separation of the LUMO from all of the other molecular orbitals. The carbene complex LUMO was found to lie 4.6 eV below the next lowest unoccupied MO, and 6.6 eV above the HOMO. The LUMO is localized on the carbene carbon: the LUMO's major component is the carbene carbon $2p_x$ orbital, which constitutes 60% of the level. The preference for nucleophilic attack at the carbene carbon could therefore be explained as a result of the spatial localization and energetic isolation of the LUMO of the complex.

In order to investigate the so-called electrophilicity of the carbene complexes with the different substituents, as described above, the molecular orbitals were calculated and the spatial localization of the chromium complex MO's are given in Figures 4.14 and 4.15. The tungsten complexes displayed similar orbitals.
For the monometallic complexes (**14**, **15**), as well as the bimetallic complexes of which the second metal was the titanium in the titanoxy substituent (**16**, **17**), the HOMO's are localized on the $M(CO)_5$-moiety, while the LUMO's are distributed across the *trans*-CO ligand, the carbene ligand as well as the delocalized ring-substituents. For complexes **18** – **21**, containing a $Cr(CO)_3$-fragment π-bonded, the $M(CO)_5$ contribution towards the HOMO's is considerably decreased, with the HOMO mostly localized on the $Cr(CO)_3$-group, although the LUMO's of these complexes exhibited the same site positions as those of the monometallic complexes.
An interesting deviation was observed for the ferrocenyl complexes (**1**, **2**) and (**5**, **6**): while the ferrocenyl ethoxycarbenes (**1**, **2**) have HOMO's distributed across both the $M(CO)_5$-moiety and the ferrocenyl group, the corresponding titanoxycarbenes (**5**, **6**) have HOMO's located almost exclusively on the $M(CO)_5$-group. This finding is in direct contrast to that of Pombeiro,[40] where the HOMO's of ferrocenyl carbene complexes encompassed both the M^0 as well as the Fe^{2+} centers. The ethoxy analogues showed a small contribution from the $M(CO)_5$-moiety with most of the HOMO situated on the ferrocenyl substituent. On the other hand, the ethoxy analogues diplayed LUMO's of the same shape as those of the aforementioned complexes, but the ferrocenyl titanoxycarbene complexes **5** and **6** are the only complexes where the LUMO is located only on the titanoxy- and carbene atoms, with no contribution from the *trans*-carbonyl ligand or the arene substituent.

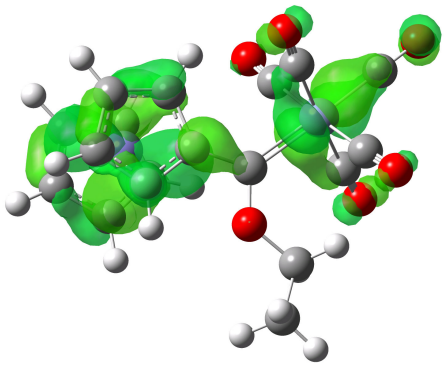

(a) **1** CrFcEt
Energy = -6.2221 eV

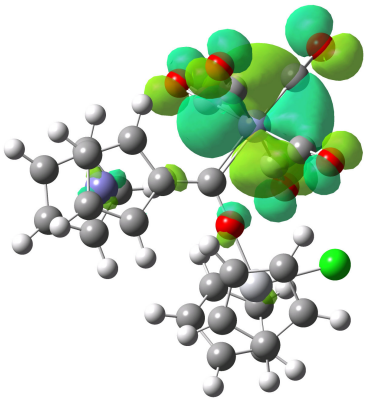

(b) **5** CrFcTi
Energy = -6.1070 eV

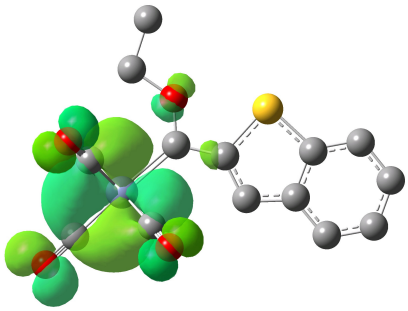

(c) **14** CrBTEt
Energy = -6.5277 eV

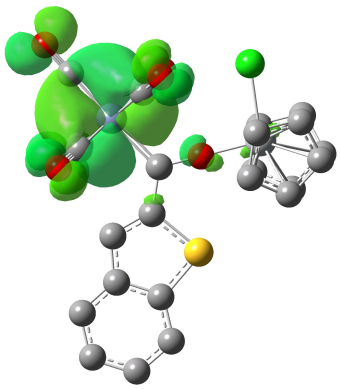

(d) **16** CrBTTi
Energy = -6.1903 eV

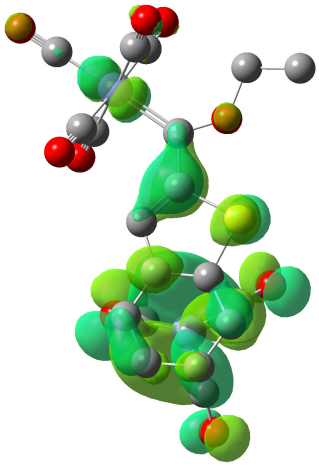

(e) **18** CrBTCrEt
Energy = -6.2420 eV

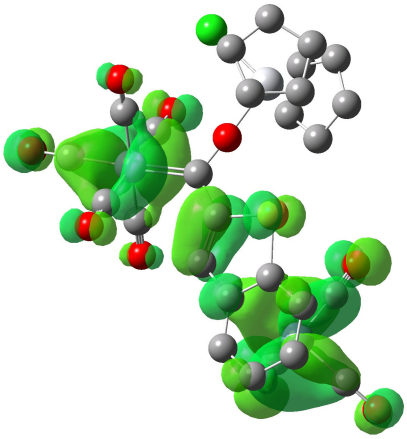

(f) **20** CrBTCrTi
Energy = -6.2918 eV

Figure 4.14 Selected HOMO representations and associated energies

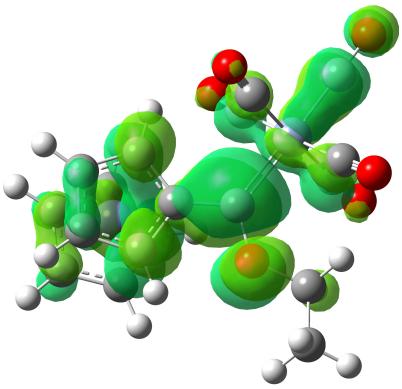

(a) **1** CrFcEt
Energy = -2.529 eV

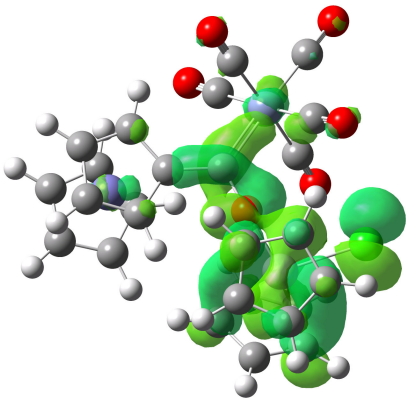

(b) **5** CrFcTi
Energy = -2.8818 eV

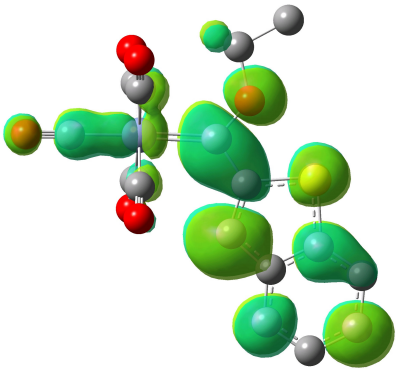

(c) **14** CrBTEt
Energy = -3.1645 eV

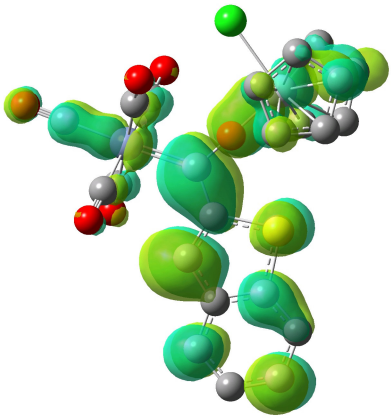

(d) **16** CrBTTi
Energy = -3.2489 eV

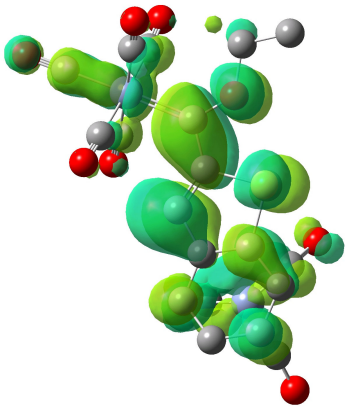

(e) **18** CrBTCrEt
Energy = -3.6244 eV

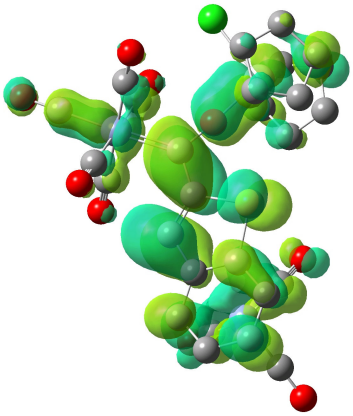

(f) **20** CrBTCrTi
Energy = -3.5833 eV

Figure 4.15 Selected LUMO representations and associated energies

As the LUMO determines the site of nucleophilic attack, [66] it seems reasonable to assume that the titanoxy *vs* ethoxy substituent will therefore greatly influence this reactivity.

To determine if the same isolation of the LUMO energy level from the other molecular orbitals calculated for a molecule also determined carbene ligand electrophilicity as observed by Block[36(a)] the energy differences between the LUMO's and the next-closest lying molecular orbitals were calculated, and are listed in Table 4.5.

Table 4.5 Molecular orbital energy differences (eV) calculated for the complexes analyzed

Complex	LUMO - HOMO	LUMO+1 - LUMO	Complex	LUMO - HOMO	LUMO+1 - LUMO
1 CrFcEt	3.6932	1.0198	**2** WFcEt	3.4818	0.6356
5 CrFcTi	3.2253	0.0460	**6** WFcTi	3.0320	0.0506
14 CrBTEt	3.3632	1.5374	**15** WBTEt	3.1335	1.0941
16 CrBTTi	2.9414	0.3320	**17** WBTTi	2.7278	0.3744
18 CrBTCrEt	2.6176	1.7387	**19** WBTCrEt	2.5308	1.3118
20 CrBTCrTi	2.7085	0.4827	**21** WBTCrTi	2.5466	0.5989

In most cases, the greatest energy separation of the LUMO from either the HOMO or the LUMO+1 energy levels were for ethoxy substituted complexes, as indicated by the blue cell in the table, while the green cells indicate differences larger than the average. For both the chromium and tungsten ferrocenyl titanoxycarbene complexes (**5** and **6**) , the calculated energy difference between the HOMO and LUMO is larger than expected, however, a very small energy difference between the LUMO and the next lowest unoccupied molecular orbital is observed, therefore not demarcating these complexes as potentially more electrophilic than the other titanoxycarbene complexes. However, this energy

difference of the HOMO and LUMO orbital energies are defined not to determine electrophilicity, but chemical hardness as defined by Pearson.[67]

Formally, as a result of the σ-donation being larger than backdonation in Fischer carbene complexes, these complexes have a $[(CO)_5Cr^{\delta-}\leftarrow C^{\delta+}]$ charge separation, which indicates lack of charge on the carbene carbon atom and also supports the electrophilic reactivity of the carbene site. Another way to evaluate the electrophilicty of these complexes is to calculate the electrophilicity index, ω, for each complex measured according to Parr, Szentpály and Liu,[68] using the expression

$$\omega \equiv \mu^2 / \eta$$

In the above equation, μ is the chemical potential[69] (the negative of the electronegativity) and η is the hardness.[67] These values are related to the molecular orbital energies, and the chemical potential and hardness can be calculated from the HOMO and LUMO orbital energies using the following approximate expressions:

$$\mu = (E_{LUMO} + E_{HOMO}) / 2$$

$$\eta = E_{LUMO} - E_{HOMO}$$

Table 4.6 Electrophilicity index of the complexes analyzed

Complex	ω (eV)	Complex	ω (eV)
1 CrFcEt	2.5919	**2** WFcEt	2.8401
5 CrFcTi	3.1315	**6** WFcTi	3.2709
14 CrBTEt	3.4915	**15** WBTEt	3.7613
16 CrBTTi	3.7864	**17** WBTTi	3.9969
18 CrBTCrEt	4.6486	**19** WBTCrEt	4.8946
20 CrBTCrTi	4.5005	**21** WBTCrTi	4.7390

[67] Pearson, R.G. *Chemical Hardness*, Wiley-VCH, Oxford, **1997**.
[68] Parr, R.G.; v. Szentpály, L.; Liu, S. *J. Am. Chem. Soc.* **1999**, *121*, 1922.
[69] Parr, R.G.; Yang, W. *Density-Functional Theory of Atoms and Molecules*, Oxford University Press, New York, **1989**.

When electrophilic indices were calculated by Frenking *et al.*[25(a)] for Fischer carbene complexes, it was found that π-donor substituents reduce the electrophilicity of the complexes, as a result of the acceptor orbital in the carbene becoming occupied by π-donation. The values listed in Table 4.6 clearly adhere to above statement. Thus for every fixed $[M(CO)_5\{C(OX)(arene)\}]$ (X = Et or $TiCp_2Cl$), the electrophilicity increases following the order Fc < 2-benzothienyl < 2-η^6-benzo[*b*]thienyl chromium tricarbonyl, demonstrating the donating properties of the ferrocenyl group, and the largest electrophilicities of the π-bonded $Cr(CO)_3$-substituted carbene complexes in line with the acceptor character of these substituents. Due to the greatly differing nature of these substituents, a greater impact on the carbene electrophilicity is effected by these ring-substituents, compared to the results of Connor[32] where the nature of the heteroatom substituent, rather than the arene-substituent or the metal, more strongly influenced the electronic nature of the carbene carbon atom.

No clear trend could be identified for the *O*-substituents. In the case of the ferrocenyl and benzothienyl complexes, higher electrophilicity indices were calculated for the titanoxy analogues. For the $[Cr(CO)_3(2\text{-}\eta^6\text{-BT})]$-substituted complexes, higher *ω*-values were obtained for the ethoxycarbene complexes, as expected from previous results where the donating character of the acyl-like oxygen of the titanoxycarbenes were proven.

4.5.5 Correlation between UV/Vis spectroscopy and MO analysis

The UV/vis spectra of complexes **5**, **6** and **18** – **21** were measured in benzene, as decomposition in chlorinated solvents, and limited solubility in hexane precluded use of these solvents. Poorly resolved spectra were obtained, thus the peak-fitting utility of the OriginPro 7.5© software programme was employed to aid in the deconvolution of the three observed absorbance peaks. Representative spectra are illustrated in Figure 4.18.

The UV-spectra of Fischer carbene complexes are known to display three well-defined absorptions: a spin-forbidden MLCT absorption at approximately 500

nm, a spin-allowed and moderately intense LF absorption in the range of 350 – 450 nm, and one additional LF transition in the range of 300 – 350 nm.[70] Strong ligand-based absorption bands occur in the range 200 – 250 nm, but were not measured during this study. The LF absorptions occurring in the 300 – 500 nm range are the π-π* transitions, where coordination to metal fragments can shift these bands to higher wavelengths. Interaction of the metal carbene π-system with that of the (hetero)aryl substituent are thus indicated by reduced energies of the π-π* transitions. The UV-visible data of the selected complexes are listed in Table 4.7, and includes energy values of the MLCT transitions in units of electron volt.

The lower energy absorption MLCT band is a metal-*d* to carbene-*p* orbital transition,[71] where the metal donates electrons to the empty *p*-orbital of the carbene carbon in the excited state, whilst the heteroatom bonded to the carbene carbon atom acts as π-donor towards the metal in the ground state (Figure 4.17). The colour of each complex is characteristic to the number of metal moieties coordinated to the ligand, and corresponds to the MLCT transition: shorter wavelength absorptions observed for the complexes displaying increasingly red colour.

Table 4.7 UV/vis data of selected complexes*

Complex	Colour	LF π-π* transition (λ, nm)	MLCT transition (λ, nm)	MLCT transition (E, eV)
5 CrFcTi	Red-brown	293, 436	504	2.460
18 CrBTCrEt	Purple	314, 471	577	2.149
20 CrBTCrTi	Dark purple	287, 509	599	2.070
6 WFcTi	Dark red	285, 427	521	2.380
19 WBTCrEt	Dark brown	323, 448	581	2.134
21 WBTCrTi	Purple	315, 480	572	2.168

* Recorded in solvent benzene

[70] Hegedus, L.S. *Tetrahedron* **1997**, *53*, 4105.
[71] Shriver, D.F.; Atkins, P.W. *Inorganic Chemistry,* 3rd Ed. Oxford University Press, Oxford, **1999**.

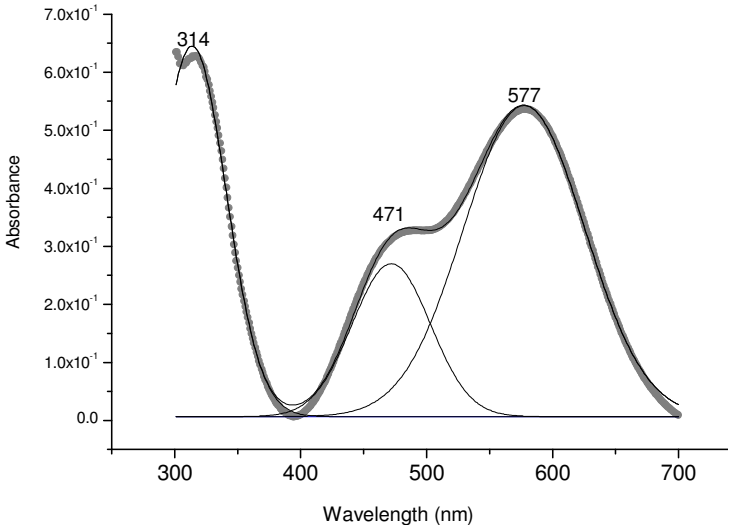

(a)

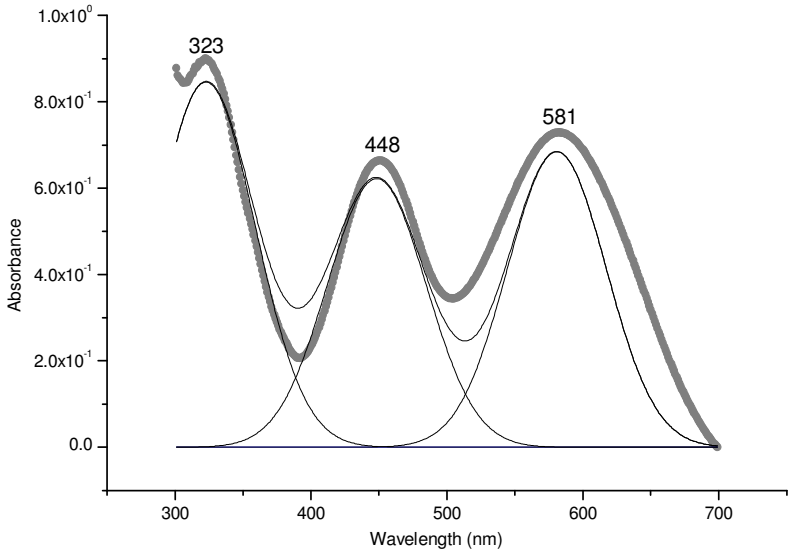

(b)

Figure 4.16 UV/vis spectra of complexes (a) **18** and (b) **19**, illustrating peak deconvolution

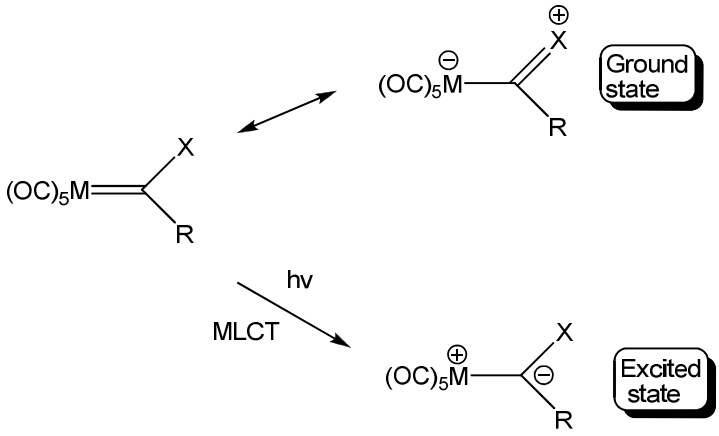

Figure 4.17 Ground and excited states in Fischer carbene complexes

The magnitude of the energies of the MLCT transitions seems to correlate more with a HOMO → LUMO transition (compare Tables 4.5 and 4.7), as described in earlier work,[36] than with the results obtained by Sierra[25(f)] where the transition was attributed to the promotion of one electron from the HOMO-1 to the LUMO. However, the UV/vis experimental work has not been corroborated by DFT calculations in this case. The size of the HOMO-LUMO energy gap can be arranged in the order CrFcTi **5** > CrBTCrEt **18** > CrBTCrTi **20**, corresponding to the inverse order of the wavelengths of the MLCT band: CrBTCrTi **20** > CrBTCrEt **18** > CrFcTi **5**. Similarly for the tungsten complexes: the HOMO-LUMO gap (eV): WFcTi **6** > WBTCrEt **19** ~ WBTCrTi **21**, and the MLCT λ (nm): WBTCrEt **19** ~ WBTCrTi **21** > WFcTi **6**.

The effect of π-accepting or donating aryl-substituents on the LF band could not be established as the arene substituents themselves varied (Fc *vs* 2-BTCr$(CO)_3$). The effect of the greater donating ability of the titanoxy fragment compared to the ethoxy group was seen in the blue shift of the π-π* transition of the ethoxycarbenes **18** and **19** (471 and 448 nm, respectively) in relation to the titanoxycarbenes **20** and **21** (509 and 480 nm, respectively).

4.5.6 Natural bond orbital analysis

The atomic orbital occupations and donor-acceptor interactions of the chromium complexes **1**, **5**, **14**, **16**, **18** and **20** were computed using the NBO method.[23] The atomic charges and orbital occupations of the relevant atoms, as indicated in Figure 4.18, participating in the metal-carbene bonding interaction, are listed in Tables 4.8 and 4.9, respectively.

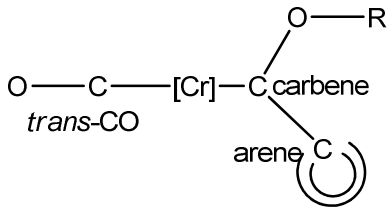

Figure 4.18 Relevant atoms and bonds (M-$CO_{trans,}$ M-$C_{carbene}$, $C_{carbene}$-C_{arene}, and $C_{carbene}$-O) analyzed by the NBO method

Table 4.8 Calculated atomic charges of selected complexes by NBO analysis

Complexes	Atomic charges			
	Cr	C(carbene)	O	C(arene)
1 CrFcEt	-1.408	+0.429	-0.555	-0.198
5 CrFcTi	-1.394	+0.453	-0.597	-0.198
14 CrBTEt	-1.401	+0.405	-0.549	-0.249
16 CrBTTi	-1.388	+0.425	-0.600	-0.243
18 CrBTCrEt	-1.400	+0.407	-0.549	-0.227
20 CrBTCrTi	-1.383	+0.427	-0.602	-0.214

The data listed in Table 4.8 only show significant variations in atomic charges on exchanging an ethoxy substituent for a titanoxy substituent, while no great effect

is observed on changing the ring-substituent, unlike the Mulliken charges listed in Table 4.4. In each case, the titanoxycarbene complex display a decreased negative charge on the chromium atom, an increased positive charge on the carbene carbon atom and an increased negative charge on the oxygen atom, demonstrating the increased ionic nature of the C(carbene)-Ti bond, so that resonance structure **I** in Figure 4.19 probably shows a greater contribution to the structure of the titanoxycarbenes, compared to their ethoxy analogues.

Table 4.9 Comparison of calculated NBO occupation of the relevant carbene ligand-associated orbitals

Calculated NBO	**1** CrFcEt	**5** CrFcTi	**14** CrBTEt	**16** CrBTTi	**18** CrBTCrEt	**20** CrBTCrTi
Cr-$C_{carbene}$ BD	-	-	1.605	1.605	1.879 1.613	1.609
Cr-$C_{carbene}$ BD*	-	-	0.486	0.500	0.646 0.472	0.486
Cr-C_{trans} BD	1.890	1.895	1.937	1.941	1.739	1.941
Cr-C_{trans} BD*	0.466	0.463	0.600	0.594	0.477	0.599
$(C\text{-}O)_{trans}$ BD	1.998 1.996 1.994	1.998 1.995 1.993	1.998 1.995 1.994	1.998 1.995 1.994	1.995 1.995	1.998 1.994 1.995
$(C\text{-}O)_{trans}$ BD*	0.189 0.170 0.016	0.189 0.170 0.016	0.187 0.167 0.016	0.188 0.168 0.016	0.050 0.149	0.184 0.016 0.163

† BD denotes a bonding orbital, BD* an antibonding orbital. Successive values denote the presence of successive bonding orbitals, therefore the presence of two BD occupation indicates a double bond.

‡ LP denotes a lone pair orbital

Table 4.9 *contd.* Comparison of calculated NBO occupation of the relevant carbene ligand-associated orbitals

Calculated NBO	**1** CrFcEt	**5** CrFcTi	**14** CrBTEt	**16** CrBTTi	**18** CrBTCrEt	**20** CrBTCrTi
$C_{carbene}$-O BD	1.987 1.974	1.987 1.932	1.988	1.987	1.987	1.987
$C_{carbene}$-O BD*	0.058 0.339	0.036 0.329	0.056	0.036	0.037	0.036
$C_{carbene}$-C_{ring} BD	1.967	1.969	1.970	1.987	1.969	1.973
$C_{carbene}$-C_{ring} BD*	0.032	0.044	0.027	0.039	0.027	0.040
O-R BD (R= Et or Ti)	1.987	1.986 1.964	1.987	-	1.987	-
O-R BD* (R= Et or Ti)	0.039	0.272 0.272	0.041	-	0.041	-
O_{trans} LP	1.973	1.974	1.974	1.974	1.974 1.546	1.974
C_{trans} LP	-	-	-	-	1.400	-
$C_{carbene}$ LP	1.403	1.376	1.406	1.378	-	1.379
O LP	1.957	-	1.953 1.717	1.745 1.644	1.952 1.714	1.780 1.757 1.637

† BD denotes a bonding orbital, BD* an antibonding orbital. Successive values denote the presence of successive bonding orbitals, therefore the presence of two BD occupation indicates a double bond.

‡ LP denotes a lone pair orbital

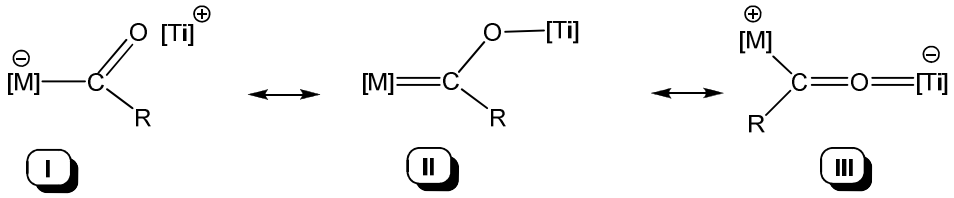

Figure 4.19 Contribution of resonance structures to the titanoxycarbene complexes

Complex **18** CrBTCrET displays the lowest electron occupation for the Cr-CO_{trans} bond, and is also the only complex exhibiting a formal Cr=C(carbene) bond with bond order of two. As seen from the experimental bond length (Table 4.1), the complex also has the shortest experimental Cr-C(carbene) bond distance. This can be ascribed to the combined electron withdrawing properties of the 2-η^6-benzo[*b*]thienyl chromium tricarbonyl substituent, and the ethoxy group which is less donating than the titanoxy group. The carbene carbon *p*-orbital also has the highest occupation, due to the greater π-donation of the central chromium towards stabilization of this electrophilic carbene carbon, thereby explaining the decreased C-O bond order of the *trans*-carbonyl ligand and its decreased electron occupation. Correspondingly, the calculated electrophilicity index ω is the highest for this complex (Table 4.6).

The ferrocenyl complexes **1** and **5** both show no formal Cr-C(carbene) bond; instead, a lone pair orbital localized on the carbene carbon atom, as well as a double bond between the C(carbene)-O atoms are obtained from NBO analysis. This correlates with the longer Cr-C(carbene) bond distances found, as the π-donor substituent ferrocenyl populates the resonance structure **B** (Scheme 4.5), shortening the C=C bond with concomitant lengthening of the Cr=C bond (Table 4.1).

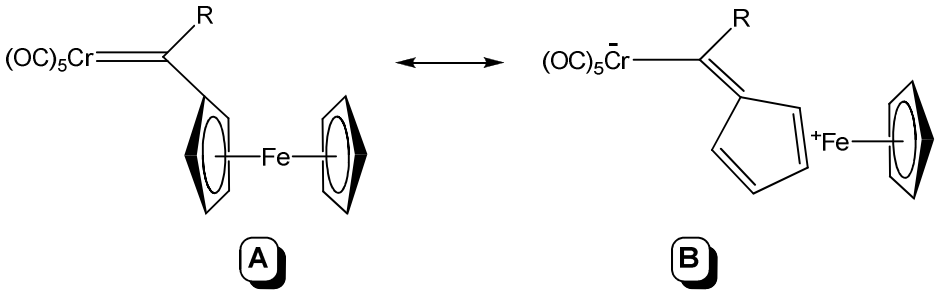

Scheme 4.5

However, no direct comparative trend for the –OEt *vs* the –$OTiCp_2Cl$ substituents can be made for a complex where the aryl-substituent is kept constant: similar occupations of the C(carbene) *p*-orbital, the Cr-C(carbene) bonding orbital and the Cr-CO_{trans} are found. Therefore, systematic prediction of the effect of different combinations of electron withdrawing and accepting substituents cannot be done. Only the results obtained for the extreme cases of accepting/least donating groups (complex **18** CrBTCrEt) or donating/donating (complex **5** CrFcTi) do correlate with the experimentally observed parameters.

4.6 Electrochemical investigation of substituent effect

Organometallic compounds that undergo rapid chemically reversible oxidation or reduction may be able to function as effective redox switches that can be turned on or off by electron transfer.[72] The chemical reactivity of the molecular system to which the redox active switch is attached can be modulated, either by electrostatic effects with the inclusion of an additional redox active metal, or by controlling the coordination environment (and reactivity) of the metal.[73]

In order to correlate the redox properties of the carbene complexes listed in Figure 4.8 with the electron donor/acceptor ability of the carbene ligands, an

[72] Yeung, L.K.; Kim, J.E.; Chung, Y.K.; Rieger, P.H.; Sweigart, D.A. *Organometallics* **1996**, *15*, 3891.
[73] Singewald, E.T.; Mirkin, C.A.; Stern, C.L. *Angew. Chem., Int. Ed. Engl.* **1995**, *34*, 1624.

investigation of the electrochemical (specifically the anodic oxidation) behaviour of these complexes were undertaken.

In a similar study of carbene and Lewis base complexes $[M(CO)_5L]$ or $[M(CO)_4L_2]$ (M = Cr, Mo or W; L = carbene ligand C(X)Y or Lewis base), it was found that the primary oxidation of these complexes corresponded to a one electron transfer.[42] In neutral compounds, the redox potential $E_{½}$ values were found to be higher when ligand L was a better π-acceptor. Increased π-conjugation within a ligand system lead to a decrease in the ease of oxidation, and increased $E_{½}$ values. In addition, for complexes $[Cr(CO)_5C(X)Y]$ the value of $E_{½}$ was not greatly influenced by Y for a specific X-group, provided that Y was an organic fragment. But if Y = Fc, redox potentials decreased by more than 200 mV. Therefore, as Y substituent became more electron donating, $E_{½}$ values decreased. Similary for decreasing donor strength of X into C(carbene) *p* orbital, increased redox potentials were observed.

4.6.1 Cyclic voltammetric studies

From the above information, it was attempted to establish a qualitative contribution of the different combinations of accepting/accepting, accepting/donating, donating/accepting and donating/donating substituents of the carbene ligands, if the substituents could be classified (for the X and Y carbene substituents, respectively) as follows: X = $OTiCp_2Cl$ (donating), X = OEt (less donating), and Y = 2-η^6-benzo[*b*]thienyl chromium tricarbonyl (accepting), Y = ferrocenyl (donating) and Y = 2-benzothienyl (less donating).

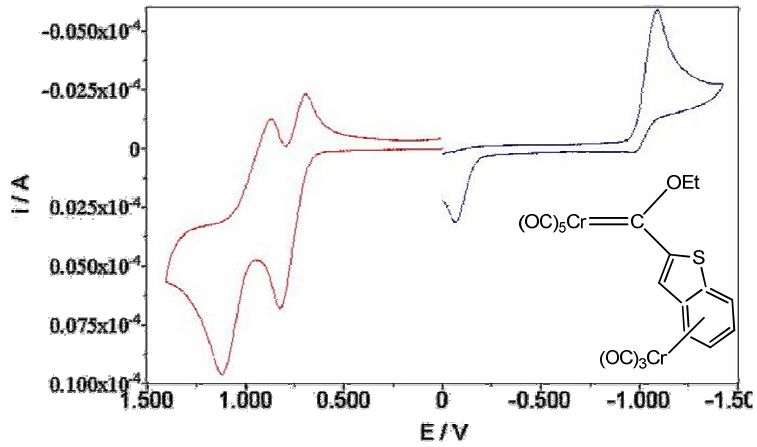

Figure 4.20 CV of 1.0 mM [$Cr(CO)_5${C(OEt)(2- η^6-benzo[*b*]thienyl-$Cr(CO)_3$)}] in CH_2Cl_2/0.10 M Bu_4NPF_6 under N_2 (g) at -75°C. The working electrode was a 1.0 mm diameter platinum disk, and the scan rate was 0.50 $V.s^{-1}$. A ferrocene internal standard had $E_{½}$ = +0.52 V

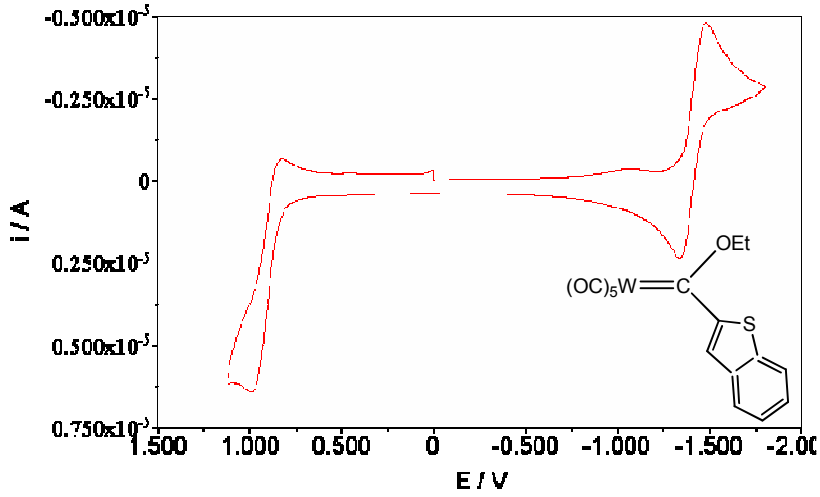

Figure 4.21 CV of 1.0 mM [$W(CO)_5${C(OEt)(2-benzothienyl)}] in CH_2Cl_2/0.10 M Bu_4NPF_6 under N_2 (g) at -75°C. The working electrode was a 1.0 mm diameter platinum disk, and the scan rate was 0.50 $V.s^{-1}$. A ferrocene internal standard had $E_{½}$ = +0.52 V

Figures 4.20 and 4.21 show typical cyclic voltammograms (CV) obtained for the complex **18** CrBTCrEt and **19** WBTEt, respectively, in CH_2Cl_2 solvent at low temperature (-75℃), and the electrochemical data is listed in Table 4.10. Full experimental details are given in the experimental section, Chapter 5.

For the chromium complexes, all reductions observed were irreversible, whereas the first reduction wave of the tungsten compounds was reversible or partially reversible. For both the chromium and tungsten complexes, the ethoxy substituted complexes only showed one cathodic wave, while the cyclic voltammograms of the titanoxycarbene complexes displayed several waves. The peak potentials of reductions are listed in Table 4.10, and are ascribed to carbene ligand-centred reductions. The titanoxycarbene complexes **16** and **20** showed irreversible cathodic waves at remarkably less negative potential (-0.95 V and -0.88 V, respectively) than the analogous ethoxycarbenes **14** and **18** with E_p = -1.21 V and -1.09 V respectively. This large potential shift can be seen as a result of the polarization of the Ti-O bond, leaving greater electron density on the oxygen atom for donating towards carbene carbon. It also serves as a possible indication of the influence of the carbene substituents on the energy of the LUMO,[46] as the LUMO's of the titanoxycarbene complexes are consistently at lower energy levels than their ethoxy counterparts observed in the molecular orbital analysis of this study.

For monometallic chromium complexes only one reversible anodic wave, corresponding to oxidation of the pentacarbonyl metal centre, is observed. The same is true for the tungsten complexes, although the oxidation waves are irreversible.

Table 4.10 Voltammetric data* and MO energies obtained for Group VI carbene complexes

Complex	Oxidation $E_{½}$ (V)	HOMO (eV)	Reduction E_c** (V)	LUMO (eV)
5 CrFcTi	+0.84 +0.62	-2.529	-1.05	-6.222
14 CrBTEt	+0.97	-3.165	-1.21	-6.528
16 CrBTTi	+0.74	-3.249	-0.95	-6.190
18 CrBTCrEt	+1.00 +0.75	-3.624	-1.09	-6.242
20 CrBTCrTi	+0.93 +0.74	-3.383	-0.88	-6.292
15 WBTEt	+1.19 †	-3.288	-1.03	-6.422
17 WBTTi	+1.03 †	-3.306	-1.05	-6.034
21 WBTCrTi	+1.11 † +0.89 †	-3.640	-1.10 -0.71	-6.186

* 1.0 mM [carbene complex] in CH_2Cl_2/0.10 M Bu_4NPF_6 under N_2 (g) at -75°C. The working electrode was a 1.0 mm diameter platinum disk, and the scan rate was 0.50 $V.s^{-1}$. A ferrocene internal standard had $E_{½}$ = +0.52 V

** E_c = peak potential of irreversible cathodic waves, or first reduction wave of reversible waves

† These values correspond to the irreversible anodic wave peak potential E_a of the tungsten complexes

For the complexes containing a second metal moiety, either Fc or 2-BTCr$(CO)_3$, another oxidation wave is observed at lower potential, showing that the two metal moieties in each complex function as separate, localized redox centres, in contrast to results obtained previously for ferrocenyl carbene complexes.[44] This implies that a direct comparison of substituent effects on the pentacarbonyl metal can be made, as it is not an electronically delocalized system. A more positive potential for CrBTCrEt **18** is obtained than for CrBTEt **14**, due to the electron withdrawing effect of the Cr$(CO)_3$-fragment in **18**, decreasing the ease of oxidation. This was also found to be valid for complex CrBTCrTi **20** *vs* CrBTTi **16**.

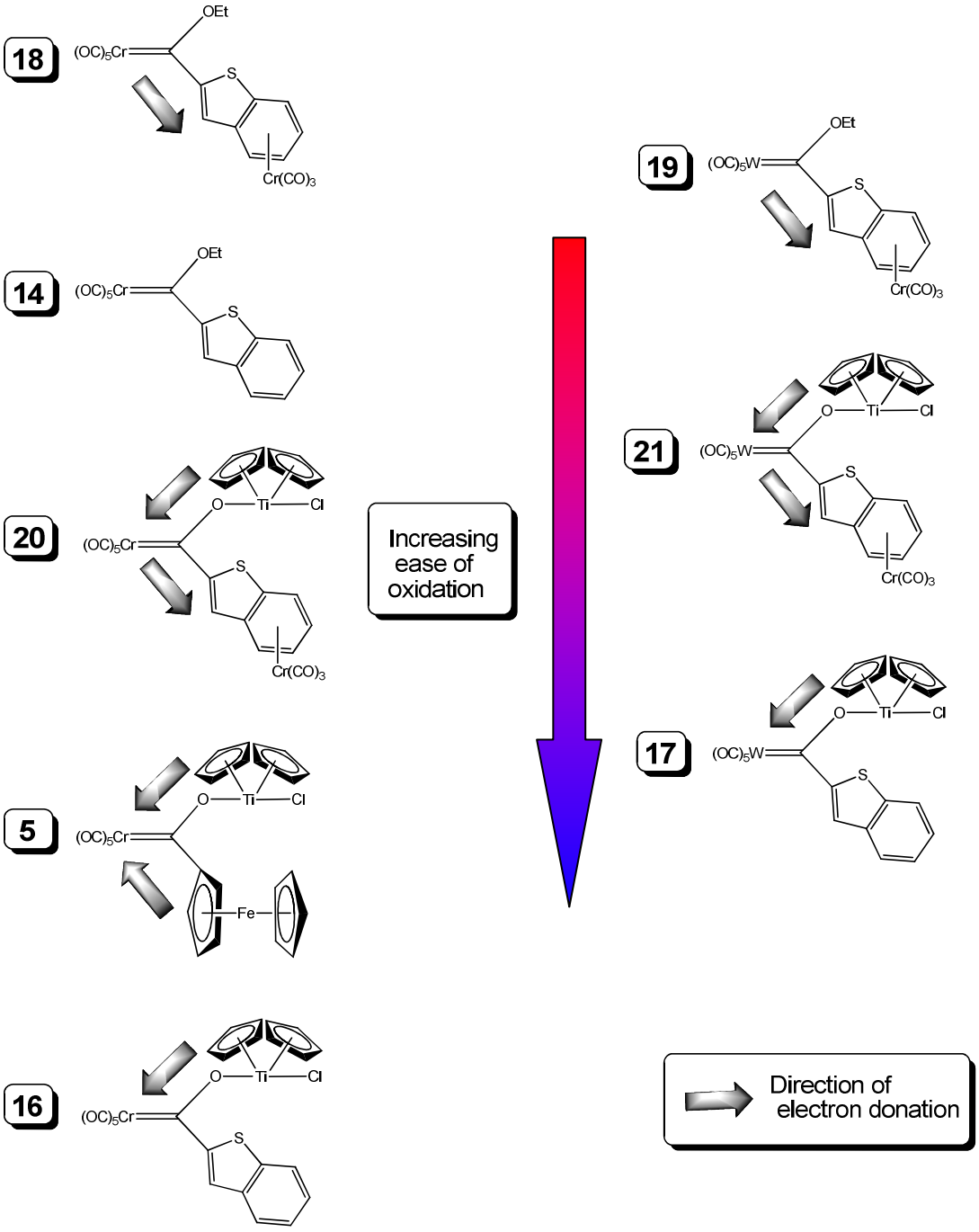

Scheme 4.6

In turn, when the –OEt *vs* –OTiCp_2Cl fragments are compared, the increased donating character of the titanoxy fragment reflects in the lower oxidation potentials obtained for these complexes **16** and **20** in relation to their ethoxy counterparts **14** and **18**. The CrFcTi complex **5** shows oxidation of the Cr-atom

at a slightly higher potential (+0.84 V) than expected compared to CrBTTi **16** (+0.74 V), as the ferrocenyl group is a stronger π-donor than the benzothienyl substituent. However, this can be rationalized by electrostatic effects: ferrocenyl complex is already oxidized at a potential of +0.62 V, localized at the iron atom. It is therefore increasingly difficult to remove a second electron from an already positively charged complex, reflecting in the higher than expected potential. The information available for the tungsten complexes reflects the same trends, and a summary of the substituent effect on oxidation potential is given in Scheme 4.6.

It is thus possible to gauge the effect of both the heteroatom substituent as well as the (hetero)arene substituent, and in addition, different combinations of the above. To combine these experimental results with the theoretical results obtained, the energies of the highest occupied molecular orbitals can be compared (Table 4.10). Except for the outlier value of the CrBTEt **14** HOMO energy, the rest of the complexes display a trend of increasing oxidation potentials corresponding to greater stability of the HOMO, as expected for a single, reversible electron removal.[45]

4.7 Concluding remarks

4.7.1 Summary

Previous studies have shown that the νCO frequencies of the carbonyl ligand *trans* to ligand L in $[M(CO)_5L]$ system does not necessarily indicate stronger or weaker π-acceptance of L, instead, correlations of π-acceptor ability with the force constants of the related carbonyl stretching frequency have been found. In this vibrational study, both νCO and calculated force constants only reflected the influence of the –OEt and $–OTiCp_2Cl$ substituents. The A_1^1 band of the carbonyl IR spectra correlated with the weakest (CrFcTi **5** and CrBTTi **16**) and strongest (CrBTCrEt **18**) M=C(carbene) bonds, but the intermediate values of the A_1' band frequencies displayed some deviations from the experimental bond lengths.

In order to remove solvent effect, solid state IR and Raman spectra were also measured. A novel $\delta CC_{carbene}O$ scissor mode was identified to directly predict the strength of the M-C(carbene) bond, and excellent correlation between the theoretically predicted frequency and observed experimental frequency was obtained. However, the inertia effects of the heavier substituents complicated assignment of the donor/acceptor properties of the carbene ligands.

Calculated electrophilicity indices ω (related to the energies of the HOMO's and LUMO's of the complexes), gave an indication of the (hetero)aromatic substituent effect, however, no conclusion about the heteroatomic substituent effect could be made. The experimental results from the UV/vis spectral data, specifically the MLCT band maxima could also be related to the magnitude of the HOMO-LUMO gap.

NBO analysis of the chromium complexes confirmed predictions about the substituent effects of the extreme cases: for the acceptor/acceptor substituted CrBTCrEt **18**, the largest bond order between the Cr-C(carbene) atoms were found, as expected for the experimentally determined shortest bond length, due to greater backdonation from the chromium towards the carbene carbon *p*-orbital. This was also reflected in the highest electron occupation of this orbital for this complex. The inverse was found for the donor/donor substituted CrFcTi **5** complex, but for the other variations of the acceptor/donor combination substituted complexes, similar occupations of the carbene carbon *p*-orbital were calculated.

The best results were obtained from the cyclic voltammetric studies, where the localized central metal redox centre's oxidation potential correlated to both the calculated HOMO energy, and the effect of both the heteroatom substituent as well as the (hetero)arene substituent, as well as different combinations of the above. Unlike the conclusion from previous studies that the electronic character of the carbene carbon atom is more strongly influenced by the X-group than either the metal or the R-group in $[M(CO)_5\{C(X)R\}]$ systems, the introduction of a third metal moiety in the R-group markedly changes the carbene character.

Carbene ligand modulation can therefore be effected by either the ring- or the heteroaromatic substituent if metal fragments are incorporated that introduces properties not available from pure organic fragments.

The substituents could be arranged in order of increasing electron withdrawing ability: ferrocenyl < 2-benzothienyl < 2-η^6-benzo[*b*]thienyl chromium tricarbonyl. The heteroatom substituents, ethoxy and titanoxy, in turn, can be arranged in order of an increasing donating effect; ethoxy < titanoxy. The arrangement of various combinations of the above (hetero)aryl and *O*-substituents (from the electrochemical analysis and HOMO energies resulted in the following trend, in order of increasing acceptor ability:

Fc, $OTiCp_2Cl$ < BT, $OTiCp_2Cl$ < $BTCr(CO)_3$, $OTiCp_2Cl$ < BT, OEt < $BTCr(CO)_3$, OEt

4.7.2 Future work

A more quantitative method of substituent analysis can be carried out by employing energy and charge decomposition analysis, where both the σ-donation between the carbene-metal bond and the π-backdonation between the metal-carbene bond and the respective contributions from these factors to the overall metal-ligand bonding situation may be established.